Brain Structure and Function (2026) 231:184
https://doi.org/10.1007/s00429-026-03241-2

ORIGINAL ARTICLE

# Comparative mapping of SATB1 expression and calcium-binding protein co-localization in the quail and pigeon brain

**Defne Albayrak[1] · Kevin B. Haselhuhn[2] · Aaron Alouane[2] · Onur Güntürkün[2,3] · Gunes Unal[1]**

Received: 26 April 2026 / Accepted: 13 November 2026
© The Author(s), under exclusive licence to Springer-Verlag GmbH Germany, part of Springer Nature 2026

## Abstract

Special AT-rich sequence-binding protein 1 (SATB1) is a genome-organizing transcription factor that promotes differentiation and survival of medial ganglionic eminence-derived parvalbumin- and somatostatin-expressing interneurons in the mammalian cortex. While SATB1 has been extensively characterized in rodents, its expression in the avian brain remains unexplored. Here, we systematically examine SATB1 immunoreactivity in the pallium and midbrain of two avian species, Japanese quail (*Coturnix japonica*) and pigeon (*Columba livia*), and its co-localization with GABA, parvalbumin, calbindin, calretinin, and secretagogin across five functionally distinct regions: the Wulst, entopallium, nidopallium caudolaterale, arcopallium, and ventral tegmental area. SATB1 sharply delineated sensory thalamorecipient zones in both species and revealed graded organizational features within the caudal nidopallium of quail and the arcopallium of pigeon. Only 4–25% of SATB1 + neurons were GABAergic, indicating that many SATB1-expressing neurons are likely glutamatergic. SATB1 and calcium-binding proteins marked largely distinct populations, with region- and species-specific exceptions. The arcopallium showed striking interspecific divergence: parvalbumin- and calretinin-positive neurons showed the greatest SATB1 overlap in quail, whereas calbindin-positive neurons showed the greatest overlap in pigeon. Parvalbumin-SATB1 co-expression in sensory pallial regions was higher in quail than pigeon, partially recapitulating the mammalian pattern. Calretinin-SATB1 co-expression across regions was a distinctive avian feature, whereas secretagogin-positive neurons showed the highest and most consistent SATB1 overlap. Together, these findings establish SATB1 as a chemoarchitectonic marker of mixed excitatory and inhibitory populations in the avian brain and reveal conserved and divergent SATB1-associated neuronal programs across amniotes.

**Keywords** SATB1 · Calcium-binding proteins · Chemoarchitecture · Pallium · Quail · Pigeon

## Introduction

Special AT-rich sequence-binding protein 1 (SATB1) is a genome-organizing transcription factor that coordinates large-scale neuronal transcriptional programs through higher-order chromatin organization (Balamotis et al. 2012). In the mammalian cortex, SATB1 is a key intrinsic regulator of inhibitory circuit development (Denaxa et al. 2012), but its expression is not restricted to GABAergic neurons. SATB1 is also expressed in subsets of excitatory pyramidal neurons of the developing neocortex, where it regulates dendritic spine density and the temporal expression of immediate early genes (Balamotis et al. 2012) and contributes to activity-dependent plasticity (Turovsky et al. 2023). During cortical development, medial ganglionic eminence (MGE)-derived interneuron precursors migrate tangentially into the cortex and subsequently mature into

Defne Albayrak and Kevin B. Haselhuhn contributed equally to this work.

✉ Gunes Unal
gunes.unal@bogazici.edu.tr

[1] Behavioral Neuroscience Laboratory, Department of Psychology, Boğaziçi University, Bebek, Istanbul 34342, Türkiye

[2] Department of Biopsychology, Institute of Cognitive Neuroscience, Faculty of Psychology, Ruhr University Bochum, Bochum, Germany

[3] Research Center One Health Ruhr, Ruhr University Bochum, Bochum, Germany

Published online: 28 November 2026

populations that include parvalbumin (PV)- and somatostatin (SST)-expressing interneurons (Hu et al. 2017; Pai et al. 2024). SATB1 is selectively upregulated in these neurons as they enter the cortical plate, acting downstream of Lhx6 and related lineage factors (Close et al. 2012; Denaxa et al. 2012; Hu et al. 2017), and promoting their terminal differentiation, connectivity, and survival (Pai et al. 2024). Accordingly, SATB1 has been widely used to identify interneuron subtypes in the rodent cortex (Viney et al. 2013), as well as neuronal subgroups in other systems such as the primate retina, including humans (Nasir-Ahmad et al. 2021). Thus, although SATB1 is strongly associated with MGE-derived interneuron identity in the mammalian cortex, its broader cellular distribution raises the question of whether this association represents a conserved feature of the vertebrate forebrain or a mammalian specialization.

In the rodent neocortex, SATB1 is expressed by overlapping but distinct subsets of PV- and SST-expressing interneurons, whereas caudal ganglionic eminence (CGE)-derived 5-HT3aR-expressing interneurons remain SATB1-negative, enabling a molecular distinction between MGE- and CGE-derived populations that is not evident from calcium-binding markers alone (Close et al. 2012). SATB1 has therefore been used both to identify specific MGE-derived interneuron cohorts and to distinguish GABAergic populations that do not engage SATB1-dependent transcriptional programs, including PV- and SST-immunopositive but SATB1-lacking axo-axonic cells in the mouse hippocampus (Viney et al. 2013). Its incorporation alongside classical cell-type biomarkers has consequently refined classification schemes of cortical interneuron diversity (Kepecs and Fishell 2014). However, these lineage-associated patterns have been established primarily in the rodent neocortex and hippocampus, and it remains unknown whether SATB1 has a similarly restricted cellular distribution outside mammals.

Historically, calcium-binding proteins such as parvalbumin, calbindin (CB), and calretinin (CR) have constituted some of the most useful biomarkers for parsing neuronal diversity in the mammalian cortex and hippocampus (Amilhon et al. 2015). PV typically labels fast-spiking interneurons that provide strong perisomatic or axon initial segment inhibition and are essential for precise spike timing (Hijazi et al. 2023). CB often marks dendrite-targeting interneurons, many of which are SST-positive, as well as specific subsets of excitatory projection neurons, whereas CR commonly labels CGE-derived interneurons that preferentially innervate other interneurons (Gulyás et al. 1996; Kepecs and Fishell 2014). More recently, secretagogin (SCGN), an EF-hand calcium-binding protein originally characterized in pancreatic and neuroendocrine cells, has been added to this panel. SCGN labels telencephalic neuronal populations largely complementary to those marked by PV, CB, and CR (Alpár et al. 2012; Mulder et al. 2009), and its cellular identity is markedly region- and species-dependent: it marks cortical GABAergic neurons of mixed ganglionic eminence origin in the human fetal telencephalon (Alzu'bi and Clowry 2020) and a subset of striatal PV+ interneurons in rats and primates, but not mice (Garas et al. 2016), whereas in the human hippocampus, SCGN immunoreactivity is confined to pyramidal neurons (Attems et al. 2007). Thus, although these markers are valuable for characterizing neuronal populations, their cellular identities can vary across regions, developmental stages, and species, and they provide limited insight into the upstream transcriptional mechanisms that shape neuronal identity (Medalla et al. 2023). In this context, examining SATB1 alongside these markers provides a complementary approach for determining the cellular populations associated with SATB1 expression and for assessing whether its relationship with inhibitory neuronal identity is conserved across vertebrate lineages.

Beyond mammals, SATB family proteins exhibit a high degree of evolutionary conservation. Cross-species analyses of SATB2 have revealed strong conservation of key functional domains across mouse, chick, and zebrafish, suggesting deeply conserved roles in forebrain development (Bhagwandin et al. 2024; Lozano et al. 2023; Medalla et al. 2023; Sheehan-Rooney et al. 2010; Tosches et al. 2018; Zhang et al. 2025). More recently, detailed analyses of SATB1 and SATB2 in bony fishes showed that these proteins retain highly conserved functional domains across sarcopterygian and actinopterygian lineages, even though their neuroanatomical expression patterns diverge significantly, indicating shared ancestral functions with lineage-specific modifications (Lozano et al. 2023). These findings indicate that SATB1-associated neuronal programs may have conserved molecular foundations across vertebrates, while their cellular distribution and functional implementation may have diverged among lineages. Birds therefore provide an important comparative system for determining whether the association between SATB1 expression and inhibitory neuronal identity observed in mammals is conserved or instead reflects lineage-specific specialization.

Birds and mammals last shared a common ancestor over 300 million years ago, yet both lineages independently evolved pallial regions that support complex cognition, including executive functions, attentional control, and flexible decision making (Güntürkün 2005; Güntürkün and Bugnyar 2016). This convergent evolution of cognitive capacity raises a fundamental question: if two vertebrate lineages achieve comparable cognitive abilities through markedly different brain architectures, a six-layered neocortex in mammals versus a nuclear pallium in birds, what molecular, neuronal, and circuit-level principles are shared across these systems?

Neuronal diversity is a fundamental feature of pallial circuit organization, and calcium-binding proteins have been widely used to characterize distinct neuronal populations across vertebrate brains. In pigeons, PV+and CB+ neurons show region-specific distributions in the somatosensory pallium, indicating substantial heterogeneity in the cellular composition of avian pallial regions (Belekhova et al. 2018). SCGN likewise identifies distinct neuronal populations in the telencephalon and midbrain of the domestic chick, complementing the distribution of canonical calcium-binding proteins (Gáti et al. 2014), and labels GAD-expressing Lugaro-like interneurons in the pigeon cerebellum (Craciun et al. 2019). More broadly, PV, CR, and CB exhibit both conserved expression patterns and interspecific variation across vertebrate brains, highlighting the evolutionary plasticity of neuronal populations defined by these markers (Hof et al. 1999; Medalla et al. 2023). However, because these markers can label heterogeneous populations across regions and species, their expression alone does not establish a common cellular identity. Determining how SATB1 expression relates to these established neuronal populations therefore provides an opportunity to assess the cellular organization and evolutionary conservation of SATB1-associated neuronal programs in the avian brain.

To address these questions, we analyzed SATB1 expression across functionally distinct pallial and midbrain regions in two avian species, the Japanese quail (*Coturnix japonica*) and the pigeon (*Columba livia*), and assessed its co-localization with the calcium-binding proteins PV, CR, CB and SCGN. The five regions selected for quantitative analysis represent key nodes of the avian cognitive network: the Wulst (hyperpallium), a primary somatosensory and visual recipient zone of the thalamofugal pathway; the entopallium, the telencephalic target of the tectofugal visual pathway; the nidopallium caudolaterale (NCL), a higher-order associative region considered a functional analogue of the mammalian prefrontal cortex; the arcopallium, a premotor and limbic output structure; and the ventral tegmental area (VTA), a midbrain dopaminergic nucleus whose projections to pallial regions modulate several executive functions. To directly characterize the cellular identity of SATB1-expressing neurons, we additionally quantified the proportion of SATB1-immunopositive cells that express GABA, allowing us to determine whether SATB1 predominantly identifies GABAergic populations or a mixed neuronal population in the avian brain. Comparing a galliform (quail) and a columbiform (pigeon) species further allowed us to distinguish lineage-specific features from patterns potentially shared across avian evolution. Together, this comparative approach characterizes SATB1 as a neuronal marker across diverse avian brain regions and provides a framework for determining which aspects of SATB1-associated neuronal organization are conserved across species and which have diverged between avian and mammalian lineages.

## Methods

### Specimen

Brain tissue was obtained from four adult pigeons (*Columba livia*) and four adult Japanese quail (*Coturnix japonica*) sourced from licensed local breeders in Istanbul, Turkey, and Bochum, Germany. All experimental procedures were approved by the Boğaziçi University Ethics Committee for the Use of Animals in Experiments (approval no. 2023-15), and were conducted in accordance with the German Animal Welfare Act and with Directive 2010/63/EU of the European Parliament and of the Council on the protection of animals used for scientific purposes.

### Tissue preparation

Animals were deeply anesthetized by intramuscular injection of ketamine (80 mg/kg body weight) combined with xylazine, and transcardially perfused with physiological saline followed by 4% depolymerized paraformaldehyde (PFA) in 0.1 M phosphate buffer (PB, pH 7.4). All procedures were performed identically in pigeons and Japanese quail. Brains were carefully removed and post-fixed in the same fixative for 48 h at 4 °C. After thorough rinsing, tissue was transferred to phosphate-buffered saline (PBS). Serial coronal Sects. (40–50 µm thickness) were obtained by using a vibrating microtome (VT1000S, Leica Microsystems, Germany). Free-floating sections were collected and stored in PBS until further processing. Brain regions were identified and delineated with reference to the stereotaxic atlas of Puelles et al. (2018) for the Japanese quail and the atlas of Halpern et al. (1967) for the pigeon.

### Immunohistochemistry

Coronal sections were processed for immunofluorescence using standard procedures with minor modifications from previously published protocols (Unal et al. 2015). Sections were washed three times for 10 min in PBS containing 0.3% Triton X-100 (PBS-Tx) to ensure adequate permeabilization. Non-specific binding was minimized by incubating sections for 1 h at room temperature in PBS-Tx containing 20% normal horse serum (NHS). Sections were then incubated for 72 h at 4 °C in PBS-Tx supplemented with 1% normal serum and the appropriate combinations of primary antibodies (refer to Table 1 for details). After primary

**Table 1** Primary antibodies

| Molecule | Host species | Dilution | Source, catalogue # | Immunogen |
|---|---|---|---|---|
| CR | Rabbit | 1:1000 | Abcam, ab92341 | Recombinant human calretinin |
| CB | Rabbit | 1:1000 | Swant, CB38 | Recombinant rat calbindin D-28k |
| PV | Rabbit | 1:1000 | Abcam, ab11427 | Native full-length protein corresponding to rat parvalbumin |
| GABA | Rabbit | 1:1000 | ThermoFisher, PA5-32241 | GABA conjugated to KLH |
| SCGN | Guinea pig | 1:1000 | Synaptic systems, 436 004 | Recombinant mouse secretagogin (amino acids 1-276) |
| SATB1 | Mouse | 1:500 | Santa Cruz, sc-376,096 | Recombinant human SATB1 |

incubation, sections were rinsed three times (10 min each) in PBS-Tx.

Fluorescent secondary antibodies including donkey anti-rabbit Alexa Fluor 488 (Thermo Fisher Scientific Cat#A-21206; 1:500), donkey anti-mouse Alexa Fluor 647 (Jackson ImmunoResearch Labs Cat#715-605-150 1:250) and donkey anti-guinea pig Alexa Fluor 405 (Jackson ImmunoResearch Labs Cat#706-475-148) were applied for 4 h at room temperature in PBS-Tx containing 1% normal serum. Following secondary incubation, sections were washed again (3 × 10 min in PBS-Tx), mounted onto gelatin-coated slides, and coverslipped using Fluoromount (Thermo Fisher Scientific). Immunohistochemical control experiments were performed by omitting the primary antibodies, which resulted in the absence of specific labeling.

## Microscopy and image acquisition

Fluorescently labeled sections were initially examined using an epifluorescence microscope (BX43, Olympus, Tokyo, Japan) equipped with a monochrome CCD camera (XM10, Olympus) and controlled via cellSens Imaging Software (version 2.2). Objective lenses included 4x (Plan Apochromat, N.A. = 0.02, dry), 10x (Plan Fluor, N.A. = 0.30, dry), and 20x (Plan Fluor, N.A. = 0.50, dry). Fluorescent signals were visualized using filter sets optimized for Alexa Fluor 405, Alexa Fluor 488, and Alexa Fluor 647.

Whole-slide and low-magnification hemisphere images were acquired using a slide-scanning microscope (Axio Scan.Z1, ZEISS, Oberkochen, Germany) equipped with an Orca Flash 4.0 V3 camera and controlled via ZEN software (ZEISS). High-resolution imaging was performed using Leica SP8 confocal microscopes (Leica Microsystems, Wetzlar, Germany) operated with LAS X software. Images were acquired using 10x (Plan Fluotar, N.A. = 0.3, dry) or 20x (Plan Fluotar, N.A. = 0.4, dry) objectives at a minimum resolution of 1024 × 1024 pixels. Fluorescent molecules were excited by the 477 nm argon laser and the 635 nm diode laser, and were detected by PMT or HyD sensors. The pinhole was set to 1 Airy unit, and for z-stack acquisition, the step size was adjusted to half the optical section thickness to ensure optimal axial resolution. All images were processed in FIJI (ImageJ; Schindelin et al. 2012), and brightness and contrast adjustments were applied uniformly across entire images without non-linear enhancement or region-specific manipulation.

## Cell quantification

Regional boundaries shown in the schematic drawings were delineated a priori according to the chick brain atlas (Puelles et al. 2018) for both species, and according to the parcellation of Herold et al. (2018) for the pigeon arcopallium/amygdala complex, guided by SATB1 immunoreactivity where it was informative (Fig. 1). SATB1 immunolabeling was not used as the sole criterion for boundary placement. For the Wulst, regions of interest encompassed the full extent of the structure without subregional differentiation. Consequently, the resulting cell counts and co-expression measures represent averages across all hyperpallial subdivisions, including the hyperpallium apicale, interstitial nucleus of the hyperpallium apicale, hyperpallium intercalatum, and hyperpallium densocellulare. Similarly, for the arcopallium, regions of interest were confined to the arcopallium proper and excluded the amygdalar subdivisions of the arcopallium/amygdala complex (Herold et al. 2018; Puelles et al. 2018).

For each animal, sections containing the regions of interest were randomly selected for analysis. For the SATB1/GABA combination, four sections per region were analyzed across the five brain regions examined (Wulst, entopallium, NCL, arcopallium, and VTA) in each species, yielding a total of 40 sections. For each calcium-binding protein combination (SATB1/PV, SATB1/CR, and SATB1/CB, SATB1/SCGN), eight sections per region per animal were analyzed across the same five brain regions, yielding a total of 240 sections. Sampling was restricted to defined anteroposterior levels for each region to ensure comparability across animals and between species. Approximate interaural levels were as follows: Wulst, A 9.5 to 11.0 mm; entopallium, A 9.0 mm; arcopallium, A 6.0 mm; NCL, A 5.5 mm; and VTA, A 4.0 mm. The interaural level sampled for each region is also provided in Table 2.

Images were first cropped to standardized regions of interest (250 × 250 µm) with brightness and contrast adjusted uniformly across images to enhance visualization while

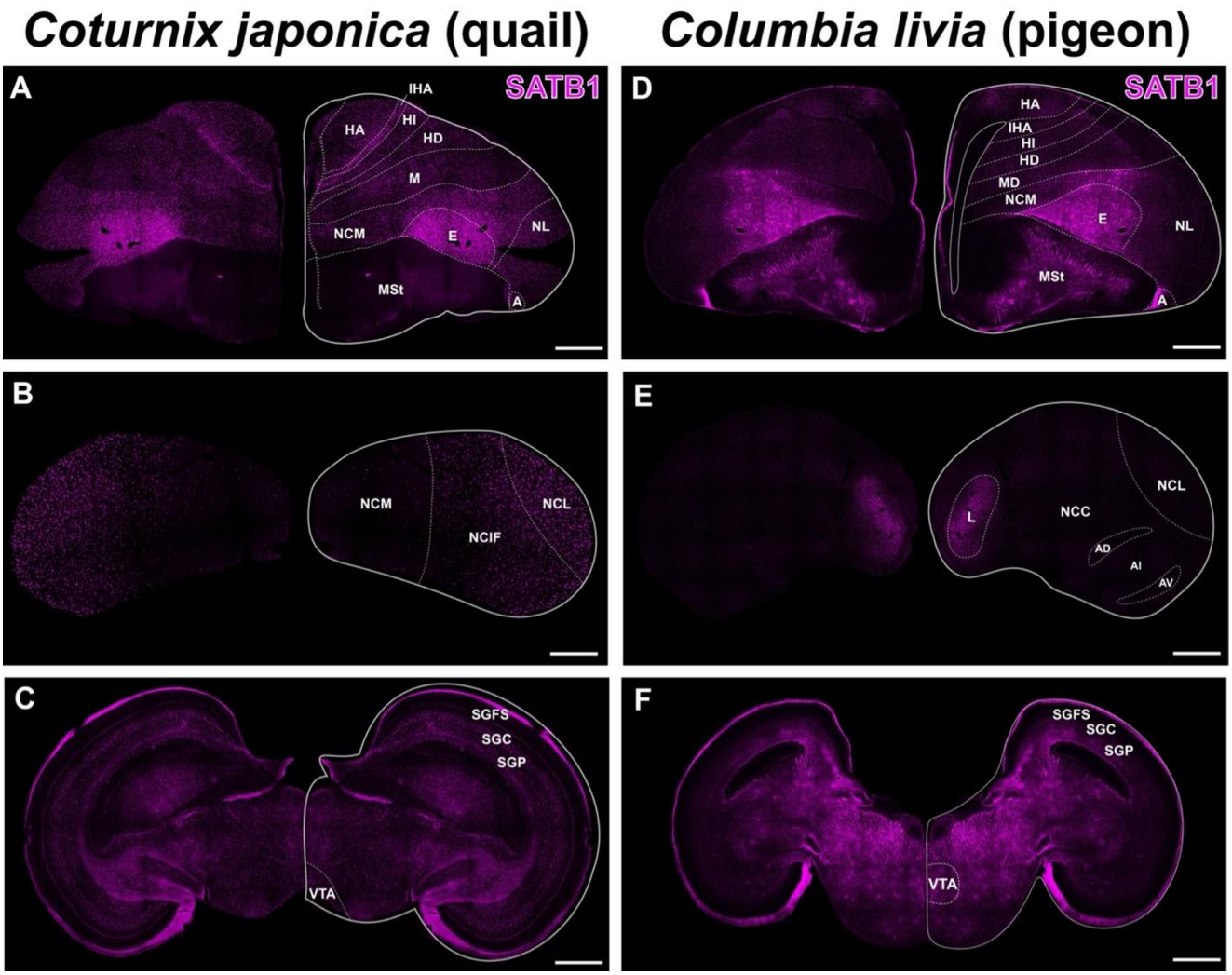



**Fig. 1** SATB1 immunoreactivity in the brain of *Coturnix japonica* (quail) and *Columba livia* (pigeon). In each panel, the left hemisphere shows the original SATB1 immunolabeling, while the opposite side presents a mirrored and annotated copy of the same hemisphere, indicating regional boundaries and labels. **A–C** Coronal sections from whole-slide scan images showing SATB1 labeling in quail at rostral telencephalic (**A**), caudal telencephalic (**B**), and midbrain (**C**) levels, with corresponding schematics illustrating major brain regions. **D–F** Matching coronal sections in pigeon at rostral telencephalic (**D**), caudal telencephalic (**E**), and midbrain (**F**) levels. A rolling ball background subtraction (radius: 800 pixels) was applied to panels C and F. *A* arcopallium; *AD* arcopallium dorsale; *AI* arcopallium intermedium; *AV* arcopallium ventrale; *E* entopallium; *HA* hyperpallium apicale; *HD* hyperpallium densocellulare; *HI* hyperpallium intercalatum; *IHA* interstitial nucleus of the hyperpallium apicale; *L* field L2; *M* mesopallium; *MD* mediopallium dorsale; *MSt* medial striatum; *NCC* nidopallium caudale pars centralis; *NCIF* nidopallium caudale island fields; *NL* nidopallium laterale; *NCM* caudomedial nidopallium; *SGC* stratum griseum centrale; *SGFS* stratum griseum et fibrosum superficiale; *SGP* stratum griseum periventriculare; *VTA* ventral tegmental area. Scale bars: 1 mm

preserving relative fluorescence intensity. Quantification of labeled cells and co-localization analyses were performed using the deep learning-based segmentation tool Cellpose (Stringer et al. 2020). Segmentation was performed using the cyto3 model in Cellpose. For SATB1 detection, the estimated cell diameter was set to 12.5 pixels, with a flow threshold of 0.4 and a cell probability threshold of 0. For GABA, PV, CR, CB and SCGN detection, the estimated cell diameter was set to 17.5 pixels, with the same flow threshold (0.4) and cell probability threshold (0). Segmentation masks were visually inspected and manually corrected when necessary to ensure accurate detection of individual somata. Total cell counts were determined by extracting unique labeled objects from the mask arrays, excluding background.

Co-localization between SATB1 and each calcium-binding protein was assessed using a custom written Python pipeline (Python 3.11; NumPy, Pandas, scikit-image, Matplotlib), as described in Albayrak et al. (2026). Briefly, segmentation masks corresponding to each marker were loaded and compared using a fast intersection over union (IoU)

**Table 2** Quantification of SATB1 co-expression with GABA and calcium-binding proteins across regions and species

| Marker | Species | Region | Level | *N* (an./sec.) | Marker+(M ± SD) | SATB1+(M ± SD) | % Mk+/SATB1 | % SATB1+/Mk |
|---|---|---|---|---|---|---|---|---|
| GABA | Quail | Wulst | A 11.0–9.5 | 4/4 | 24.0 ± 7.3 | 136.8 ± 45.1 | 18.7 ± 9.7 | 4.2 ± 3.3 |
| GABA | Quail | Ento | A 9.0 | 4/4 | 43.2 ± 15.3 | 172.5 ± 10.0 | 17.7 ± 10.2 | 5.1 ± 4.9 |
| GABA | Quail | NCL | A 5.5 | 4/ 4 | 48.8 ± 19.9 | 76.2 ± 34.5 | 37.2 ± 26.7 | 10.4 ± 6.9 |
| GABA | Quail | Arco | A 6.0 | 4/4 | 60.5 ± 12.2 | 40.8 ± 34.6 | 11.6 ± 4.8 | 24.3 ± 19.3 |
| GABA | Quail | VTA | A 4.0 | 4/4 | 46.5 ± 14.8 | 17.2 ± 7.5 | 4.6 ± 4.0 | 13.5 ± 10.4 |
| GABA | Pigeon | Wulst | A 11.0–9.5 | 4/4 | 30.5 ± 7.4 | 99.2 ± 16.5 | 23.4 ± 9.9 | 10.0 ± 3.7 |
| GABA | Pigeon | Ento | A 9.0 | 4/4 | 61.0 ± 7.6 | 164.2 ± 26.3 | 13.2 ± 6.4 | 5.5 ± 1.9 |
| GABA | Pigeon | NCL | A 5.5 | 4/4 | 36.8 ± 4.5 | 123.0 ± 14.9 | 28.0 ± 16.2 | 8.8 ± 4.7 |
| GABA | Pigeon | Arco | A 6.0 | 4/4 | 58.0 ± 14.7 | 91.5 ± 28.7 | 28.1 ± 13.3 | 10.7 ± 2.3 |
| GABA | Pigeon | VTA | A 4.0 | 4/4 | 69.0 ± 13.8 | 17.5 ± 3.7 | 6.5 ± 3.4 | 20.8 ± 9.3 |
| PV | Quail | Wulst | A 11.0–9.5 | 4/8 | 25.6 ± 17.7 | 147.1 ± 40.9 | 51.0 ± 39.4 | 13.0 ± 12.7 |
| PV | Quail | Ento | A 9.0 | 4/8 | 15.0 ± 11.9 | 105.0 ± 24.9 | 45.5 ± 34.3 | 11.7 ± 15.1 |
| PV | Quail | NCL | A 5.5 | 4/8 | 4.2 ± 3.0 | 62.4 ± 20.5 | 37.7 ± 38.5 | 3.0 ± 3.7 |
| PV | Quail | Arco | A 6.0 | 4/8 | 3.7 ± 2.1 | 51.3 ± 28.5 | 51.9 ± 35.8 | 7.9 ± 11.0 |
| PV | Quail | VTA | A 4.0 | 4/8 | 10.2 ± 8.6 | 21.3 ± 10.5 | 4.7 ± 7.7 | 1.8 ± 3.0 |
| PV | Pigeon | Wulst | A 11.0–9.5 | 4/8 | 10.6 ± 5.4 | 124.2 ± 44.2 | 18.8 ± 21.0 | 1.5 ± 1.3 |
| PV | Pigeon | Ento | A 9.0 | 4/8 | 6.1 ± 4.7 | 132.7 ± 27.7 | 14.5 ± 21.6 | 1.9 ± 4.1 |
| PV | Pigeon | NCL | A 5.5 | 4/8 | 8.3 ± 6.3 | 43.8 ± 27.5 | 10.3 ± 13.1 | 4.5 ± 7.4 |
| PV | Pigeon | Arco | A 6.0 | 4/8 | 9.0 ± 3.7 | 57.1 ± 15.7 | 7.1 ± 13.4 | 1.0 ± 1.6 |
| PV | Pigeon | VTA | A 4.0 | 4/8 | 9.5 ± 4.9 | 13.9 ± 6.0 | 8.2 ± 11.5 | 6.0 ± 7.1 |
| CR | Quail | Wulst | A 11.0–9.5 | 4/8 | 19.4 ± 7.0 | 131.9 ± 10.9 | 32.6 ± 18.4 | 5.8 ± 3.7 |
| CR | Quail | Ento | A 9.0 | 4/8 | 12.2 ± 12.0 | 118.4 ± 48.6 | 40.3 ± 26.5 | 3.7 ± 3.1 |
| CR | Quail | NCL | A 5.5 | 4/8 | 19.4 ± 10.8 | 65.2 ± 32.7 | 54.0 ± 22.4 | 7.6 ± 4.0 |
| CR | Quail | Arco | A 6.0 | 4/8 | 17.5 ± 14.3 | 57.5 ± 33.8 | 68.6 ± 23.1 | 8.5 ± 6.0 |
| CR | Quail | VTA | A 4.0 | 4/8 | 14.3 ± 7.4 | 9.6 ± 4.9 | 14.2 ± 16.1 | 17.9 ± 17.2 |
| CR | Pigeon | Wulst | A 11.0–9.5 | 4/8 | 81.5 ± 32.1 | 135.4 ± 55.2 | 34.2 ± 14.0 | 44.0 ± 19.9 |
| CR | Pigeon | Ento | A 9.0 | 4/8 | 14.7 ± 14.9 | 156.5 ± 41.6 | 37.0 ± 10.0 | 7.6 ± 12.1 |
| CR | Pigeon | NCL | A 5.5 | 4/8 | 16.6 ± 9.0 | 59.9 ± 54.0 | 36.1 ± 30.7 | 11.1 ± 6.8 |
| CR | Pigeon | Arco | A 6.0 | 4/8 | 18.7 ± 12.6 | 58.4 ± 44.6 | 32.5 ± 23.1 | 15.4 ± 13.7 |
| CR | Pigeon | VTA | A 4.0 | 4/8 | 8.0 ± 2.6 | 7.0 ± 7.0 | 6.1 ± 10.5 | 4.4 ± 7.7 |
| CB | Quail | Wulst | A 11.0–9.5 | 4/8 | 16.7 ± 12.6 | 146.4 ± 55.2 | 43.4 ± 23.4 | 4.4 ± 2.5 |
| CB | Quail | Ento | A 9.0 | 4/8 | 21.4 ± 17.6 | 120.3 ± 52.2 | 34.9 ± 28.8 | 9.5 ± 9.1 |
| CB | Quail | NCL | A 5.5 | 4/8 | 33.7 ± 20.8 | 71.7 ± 54.1 | 29.6 ± 24.8 | 13.6 ± 10.8 |
| CB | Quail | Arco | A 6.0 | 4/8 | 19.5 ± 19.0 | 61.3 ± 46.8 | 22.7 ± 20.4 | 6.8 ± 7.8 |
| CB | Quail | VTA | A 4.0 | 4/8 | 13.0 ± 14.8 | 15.8 ± 12.4 | 14.8 ± 8.0 | 13.0 ± 10.9 |
| CB | Pigeon | Wulst | A 11.0–9.5 | 4/8 | 9.2 ± 4.8 | 143.3 ± 49.5 | 32.8 ± 23.7 | 3.7 ± 5.1 |
| CB | Pigeon | Ento | A 9.0 | 4/8 | 6.2 ± 3.0 | 169.9 ± 40.6 | 36.1 ± 27.3 | 1.0 ± 0.9 |
| CB | Pigeon | NCL | A 5.5 | 4/8 | 36.9 ± 19.4 | 62.7 ± 55.7 | 31.1 ± 12.2 | 13.5 ± 6.5 |
| CB | Pigeon | Arco | A 6.0 | 4/8 | 14.2 ± 11.0 | 64.2 ± 19.5 | 45.8 ± 21.3 | 10.7 ± 10.6 |
| CB | Pigeon | VTA | A 4.0 | 4/8 | 9.3 ± 2.8 | 6.7 ± 3.8 | 2.4 ± 4.1 | 5.2 ± 9.7 |
| SCGN | Quail | Wulst | A 11.0–9.5 | 4/8 | 19.5 ± 0.7 | 138.5 ± 38.9 | 51.6 ± 16.4 | 7.8 ± 4.2 |
| SCGN | Quail | Ento | A 9.0 | 4/8 | 7.0 ± 5.7 | 127.0 ± 24.0 | 31.8 ± 45.0 | 2.4 ± 3.4 |
| SCGN | Quail | NCL | A 5.5 | 4/8 | 20.5 ± 7.8 | 111.0 ± 2.8 | 66.5 ± 9.3 | 12.5 ± 6.1 |
| SCGN | Quail | Arco | A 6.0 | 4/8 | 15.0 ± 2.8 | 50.5 ± 31.8 | 15.4 ± 21.8 | 2.7 ± 3.9 |
| SCGN | Quail | VTA | A 4.0 | 4/8 | 5.5 ± 3.5 | 11.0 ± 0.0 | 0.0 ± 0.0 | 0.0 ± 0.0 |
| SCGN | Pigeon | Wulst | A 11.0–9.5 | 4/8 | 22.0 ± 8.5 | 259.5 ± 3.5 | 74.1 ± 16.4 | 6.5 ± 3.7 |
| SCGN | Pigeon | Ento | A 9.0 | 4/8 | 10.0 ± 11.3 | 115.5 ± 23.3 | 36.1 ± 19.6 | 2.0 ± 1.4 |
| SCGN | Pigeon | NCL | A 5.5 | 4/8 | 5.0 ± 1.4 | 146.0 ± 15.6 | 58.3 ± 11.8 | 2.0 ± 0.8 |
| SCGN | Pigeon | Arco | A 6.0 | 4/8 | 10.0 ± 7.1 | 33.5 ± 12.0 | 3.3 ± 4.7 | 2.0 ± 2.8 |
| SCGN | Pigeon | VTA | A 4.0 | 4/8 | 6.5 ± 0.7 | 2.0 ± 0.0 | 8.3 ± 11.8 | 25.0 ± 35.4 |

Values are mean (M) ± standard deviation (SD) of per-section cell counts. n, number of animals/sections analyzed. Marker + and SATB1 + denote mean immunopositive cell counts per section. % Mk+/SATB1, percentage of marker-positive cells co-expressing SATB1; % SATB1+/Mk, percentage of SATB1-positive cells co-expressing the marker. All counts were obtained from the left hemisphere. *Arco* arcopallium; *NCL* nidopallium caudolaterale; *Ento* entopallium; *VTA* ventral tegmental area

based matching approach. Pixelwise intersections between labeled objects were computed, and IoU values were calculated as the ratio of intersection area to union area for each potential object pair. A greedy one to one matching algorithm was applied, ranking candidate pairs by descending IoU score and assigning matches only when IoU ≥ 0.20. Each segmented object was allowed to match only one partner to prevent duplicate assignments.

Each marker combination (SATB1/PV, SATB1/CR, SATB1/CB, SATB1/SCGN) was processed in an independent double-labeling series on separate sections. Absolute SATB1 labeling intensity is therefore not directly comparable across Figs. 2, 3, 4, 5 and 6, and only the co-expression relationships quantified within each series are interpreted. For each section, we quantified the total number of double-labeled cells and calculated the overlap between SATB1 + cells and PV+, CR+, CB + or SCGN+ populations. Because these markers label populations of markedly different absolute sizes, co-expression was assessed using two complementary measures: the proportion of calcium-binding protein positive (PV+, CR+, CB + or SCGN+) neurons that also expressed SATB1, and the proportion of SATB1 + neurons that also expressed the respective marker. Overlap percentages were calculated by dividing the number of double-labeled cells by either the total number of calcium-binding protein positive cells or the total number of SATB1 + cells, and multiplying by 100. Per-region cell counts and co-expression percentages for all markers are summarized in Table 2.

## Results

### SATB1 distribution in quail brain

Immunohistochemical analysis revealed a distinctive and region-specific pattern of SATB1 expression across the pallium of the Japanese quail (Fig. 1A–C). At rostral

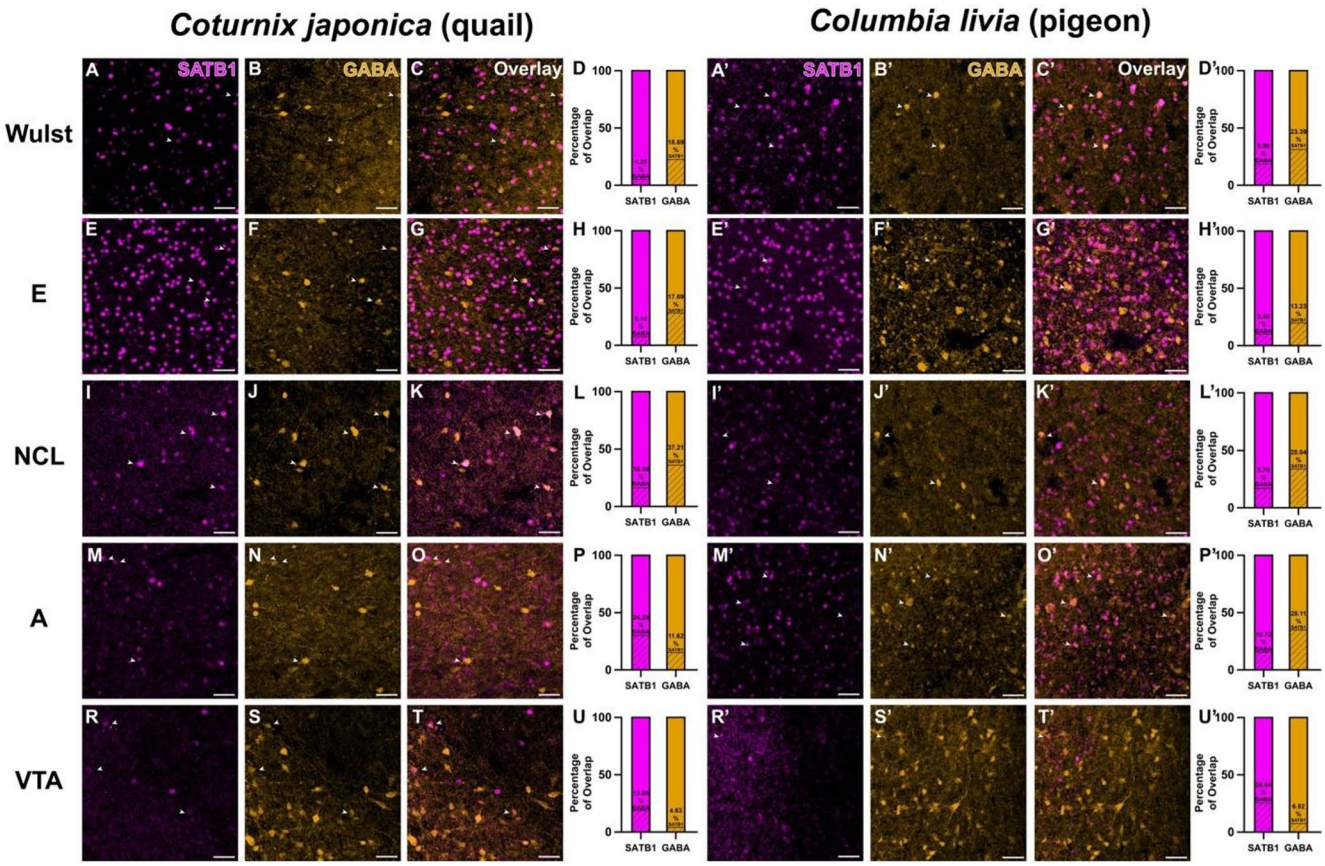



**Fig. 2** GABA and SATB1 co-expression across pallial and midbrain regions in quail and pigeon. **A–U** Confocal images from quail showing SATB1 (**A**, **E**, **I**, **M**, **R**; magenta), GABA (**B**, **F**, **J**, **N**, **S**; yellow), and merged channels (**C**, **G**, **K**, **O**, **T**), together with stacked bar graphs showing marker co-expression (**D**, **H**, **L**, **P**, **U**). In each graph, the left bar indicates the proportion of SATB1 + cells co-expressing GABA, and the right bar indicates the proportion of GABA+ cells co-expressing SATB1. **A'–U'** Corresponding confocal images and bar graphs from pigeon. Arrowheads indicate representative double-labeled (SATB1+/GABA+) neurons. A 1-pixel median filter was applied to all confocal images for noise reduction. Rows from top to bottom show the Wulst, entopallium (E), nidopallium caudolaterale (NCL), arcopallium (A), and ventral tegmental area (VTA). Scale bars: 50 µm

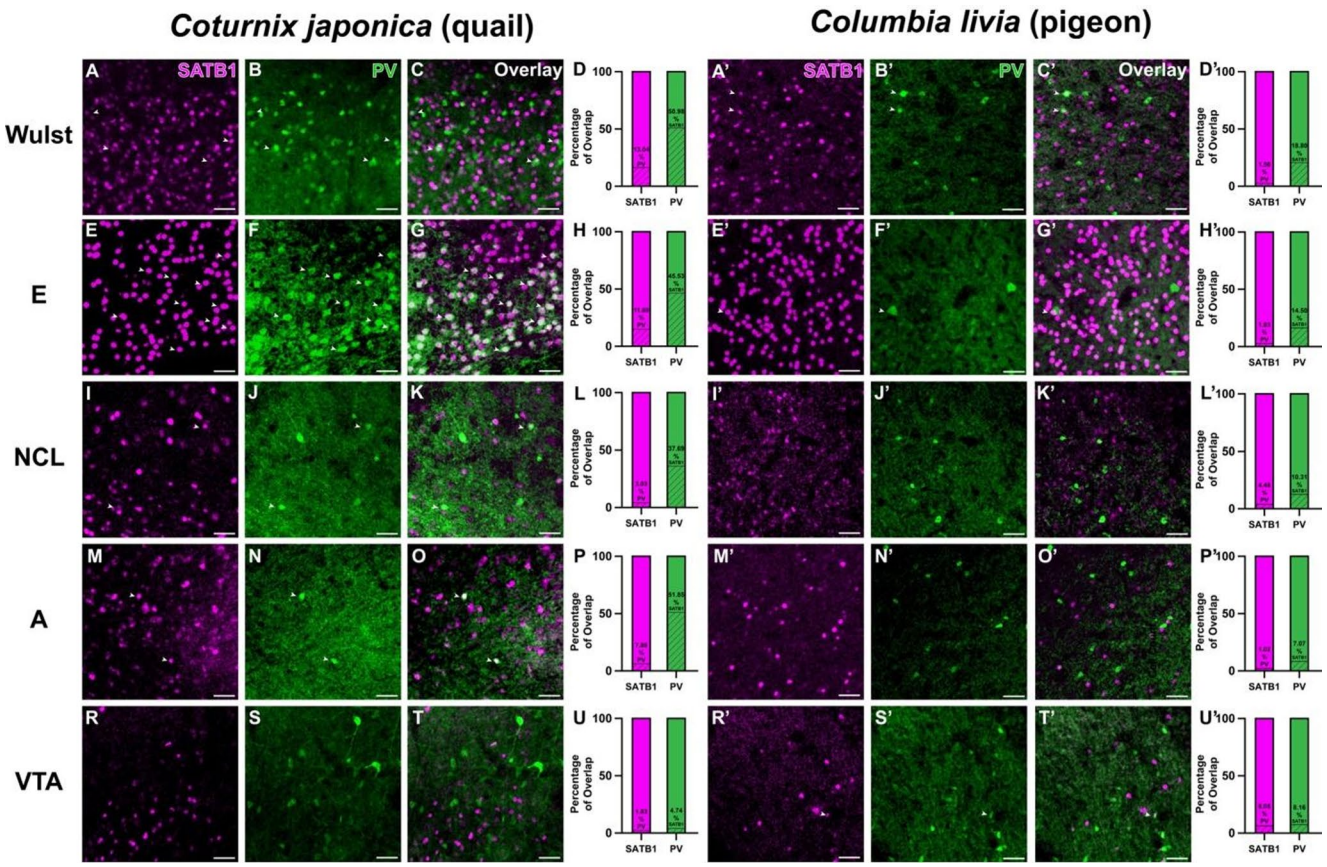



**Fig. 3** PV and SATB1 co-expression across pallial and midbrain regions in quail and pigeon. **A–U** Confocal images from quail showing SATB1 (**A**, **E**, **I**, **M**, **R**; magenta), PV (**B**, **F**, **J**, **N**, **S**; green), and merged channels (**C**, **G**, **K**, **O**, **T**), together with stacked bar graphs showing marker co-expression (**D**, **H**, **L**, **P**, **U**). In each graph, the left bar indicates the proportion of SATB1 + cells co-expressing PV, and the right bar indicates the proportion of PV+ cells co-expressing SATB1. **A'–U'** Corresponding confocal images and bar graphs from pigeon. Arrowheads indicate representative double-labeled (SATB1+/PV+) neurons. A 1-pixel median filter was applied to all confocal images for noise reduction. Rows from top to bottom show the Wulst, entopallium (E), nidopallium caudolaterale (NCL), arcopallium (A), and ventral tegmental area (VTA). Scale bars: 50 µm

telencephalic levels, SATB1 immunoreactivity prominently delineated the entopallium, where a high density of immunopositive neurons produced a band of labeling that clearly demarcated this thalamorecipient sensory structure from the surrounding pallial territories (Fig. 1A). The moderately higher SATB1 density in the entopallium relative to the surrounding nidopallium produced a recognizable boundary, supporting SATB1 as a useful chemoarchitectonic marker for this structure in quail.

SATB1 expression within the Wulst was concentrated in the interstitial nucleus of the hyperpallium apicale (IHA), a thalamorecipient layer characterized by densely packed granular neurons, where numerous immunopositive somata were observed. This expression pattern distinguished the IHA from the immediately adjacent hyperpallium intercalatum (HI), as well as from the more ventral hyperpallium densocellulare (HD) and the mesopallium (M), all of which exhibited sparse and faint SATB1 immunoreactivity (Fig. 1A). The differential expression across these Wulst subdivisions indicates that SATB1 captures a molecular boundary between the IHA and its neighboring pallial fields that is not always evident in previous cytoarchitectonic analyses.

The arcopallium proper exhibited moderate levels of SATB1 expression, with immunopositive neurons distributed at intermediate density. Within the arcopallium/amygdala complex, SATB1 labeling appeared to be concentrated in the arcopallium proper rather than in the amygdalar subareas (Herold et al. 2018).

At caudal telencephalic levels, a clear regional gradient was observed within the nidopallium (Fig. 1B). The caudomedial nidopallium (NCM), an auditory associative region occupying the medial aspect of the caudal telencephalon, was virtually negative for SATB1, with only rare, faintly labeled cells observed against an otherwise unlabeled background. The nidopallium caudale island fields (NClF), situated between the NCM and NCL, exhibited a clear lateral-to-medial gradient of SATB1 expression,

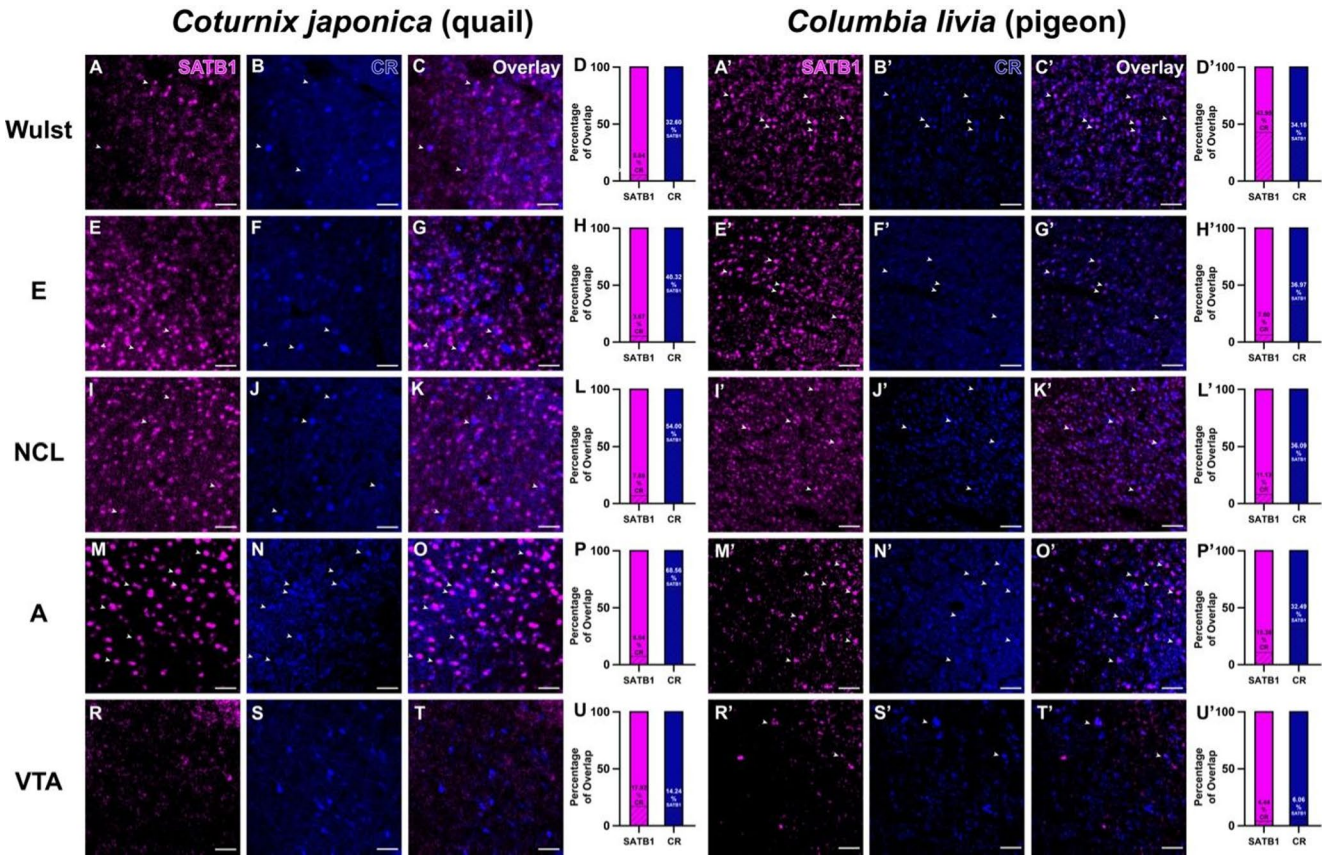



**Fig. 4** CR and SATB1 co-expression across pallial and midbrain regions in quail and pigeon. **A–U** Confocal images from quail showing SATB1 (**A**, **E**, **I**, **M**, **R**; magenta), CR (**B**, **F**, **J**, **N**, **S**; blue), and merged channels (**C**, **G**, **K**, **O**, **T**), together with stacked bar graphs showing marker co-expression (**D**, **H**, **L**, **P**, **U**). In each graph, the left bar indicates the proportion of SATB1 + cells co-expressing CR, and the right bar indicates the proportion of CR+ cells co-expressing SATB1. **A'–U'** Corresponding confocal images and bar graphs from pigeon. Arrowheads indicate representative double-labeled (SATB1+/CR+) neurons. A 1-pixel median filter was applied to all confocal images for noise reduction. Rows from top to bottom show the Wulst, entopallium (E), nidopallium caudolaterale (NCL), arcopallium (A), and ventral tegmental area (VTA). Scale bars: 50 µm

with labeling decreasing toward the medial border adjoining the NCM. In sharp contrast, the NCL showed abundant SATB1 expression with densely packed immunopositive neurons (Fig. 1B). The observed medial to lateral gradient of increasing SATB1 density across NCM, NClF, and NCL suggests that SATB1 expression delineates functionally distinct subdivisions within the caudal nidopallium of the quail. The medial striatum (MSt) was largely devoid of SATB1 immunoreactivity, appearing as a dark territory in the ventromedial telencephalon. The absence of labeling in this subpallial region provided a useful internal reference delimiting the pallial/subpallial boundary.

Beyond the telencephalon, SATB1 robustly labeled the optic tectum (Tect), where a high density of immunoreactive neurons was distributed across its layered architecture (Fig. 1C). The intensity of tectal labeling was among the strongest observed in the entire quail brain. SATB1 + neurons were visible across multiple tectal layers. The densest labeling formed a prominent band in the stratum griseum centrale (SGC), with additional labeled neurons in the deep sublayers of the stratum griseum et fibrosum superficiale (SGFS). A thinner band of labeled cells was also present in the superficial sublayers of the SGFS, and scattered cells were observed in the stratum griseum periventriculare (SGP), producing an overall laminar pattern readily discernible at low magnification. A cluster of SATB1 + neurons was also observed in the central midbrain in a position consistent with the avian equivalent of torus semicircularis. The VTA showed moderate SATB1 expression, with a scattered population of immunopositive neurons that were considerably sparser than in the overlying tectum (Fig. 1C).

## SATB1 distribution in pigeon brain

The pigeon pallium exhibited a SATB1 expression pattern that shared certain features with the quail, while also displaying notable species-specific differences (Fig. 1D–G). As in quail, SATB1 immunoreactivity clearly delineated

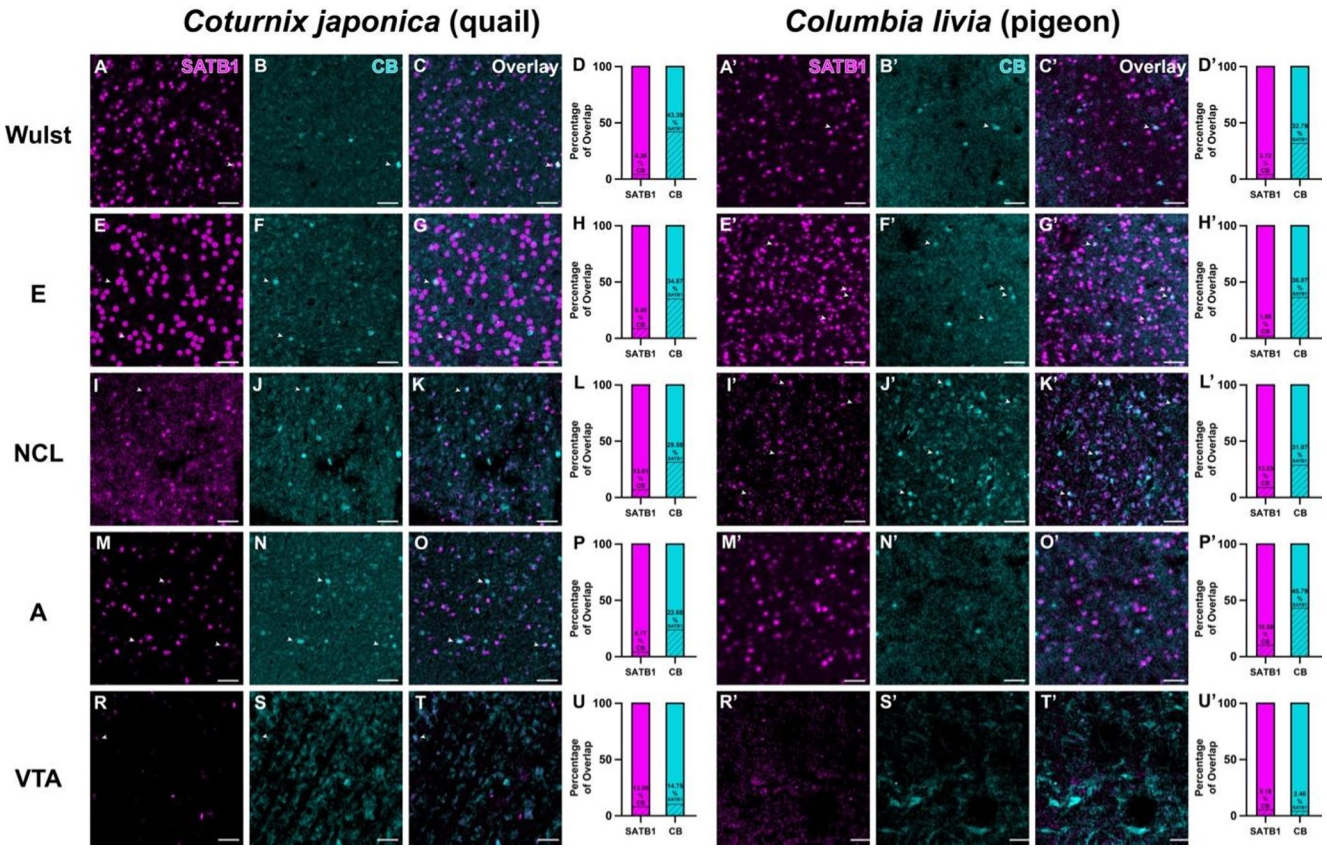



**Fig. 5** CB and SATB1 co-expression across pallial and midbrain regions in quail and pigeon. **A–U** Confocal images from quail showing SATB1 (**A**, **E**, **I**, **M**, **R**; magenta), CB (**B**, **F**, **J**, **N**, **S**; cyan), and merged channels (**C**, **G**, **K**, **O**, **T**), together with stacked bar graphs showing marker co-expression (**D**, **H**, **L**, **P**, **U**). In each graph, the left bar indicates the proportion of SATB1 + cells co-expressing CB, and the right bar indicates the proportion of CB+ cells co-expressing SATB1. **A'–U'** Corresponding confocal images and bar graphs from pigeon. Arrowheads indicate representative double-labeled (SATB1+/CB+) neurons. A 1-pixel median filter was applied to all confocal images for noise reduction. Rows from top to bottom show the Wulst, entopallium (E), nidopallium caudolaterale (NCL), arcopallium (A), and ventral tegmental area (VTA). Scale bars: 50 µm

the entopallium, where a dense population of immunopositive neurons demarcated this visual area as a well-defined domain within the nidopallium, ventral to the mesopallium (Fig. 1D). The entopallial labeling was distinguishable from the lower SATB1 signal in the immediately surrounding nidopallium and mesopallium, confirming the utility of SATB1 as an entopallial boundary marker across both species examined.

Within the Wulst, the IHA contained a dense layer of SATB1 + neurons, situated beneath the HA, which showed relatively minimal expression (Fig. 1D). SATB1 labeling also marked the transition zone between the caudomedial nidopallium (NCM) and the mesopallium dorsale (MD). The MD and NCM both displayed low SATB1 immunoreactivity although MD had more SATB1 + cells and these territories were clearly separated by a cell free lamina (Fig. 1D).

A particularly striking feature of the pigeon pallium was the high SATB1 expression that defined field L2 (L), the primary auditory thalamorecipient zone within the nidopallium (Fig. 1E). This structure appeared as a densely labeled ovoid domain in which the concentration of immunopositive neurons was among the highest observed in pigeon telencephalon. The intense labeling sharply delineated field L2 from the surrounding caudonidopallial territory, including the nidopallium caudale, pars centralis (NCC), which displayed comparatively low to moderate SATB1 signal (Fig. 1E). Notably, all three thalamopallial sensory input zones examined across both species, the entopallium, the IHA, and field L2, displayed high SATB1 expression, suggesting that strong SATB1 immunoreactivity may be a shared molecular feature of primary sensory thalamorecipient areas in the avian pallium.

In marked contrast to the quail, where the NCL was one of the most densely labeled pallial regions, the NCL of the pigeon exhibited comparatively lower SATB1 immunoreactivity, with a more dispersed and less intensely labeled population of cells scattered throughout this executive region (Fig. 1E). This interspecific difference in NCL expression represents one of the most apparent divergences in SATB1 distribution between the two avian species examined and

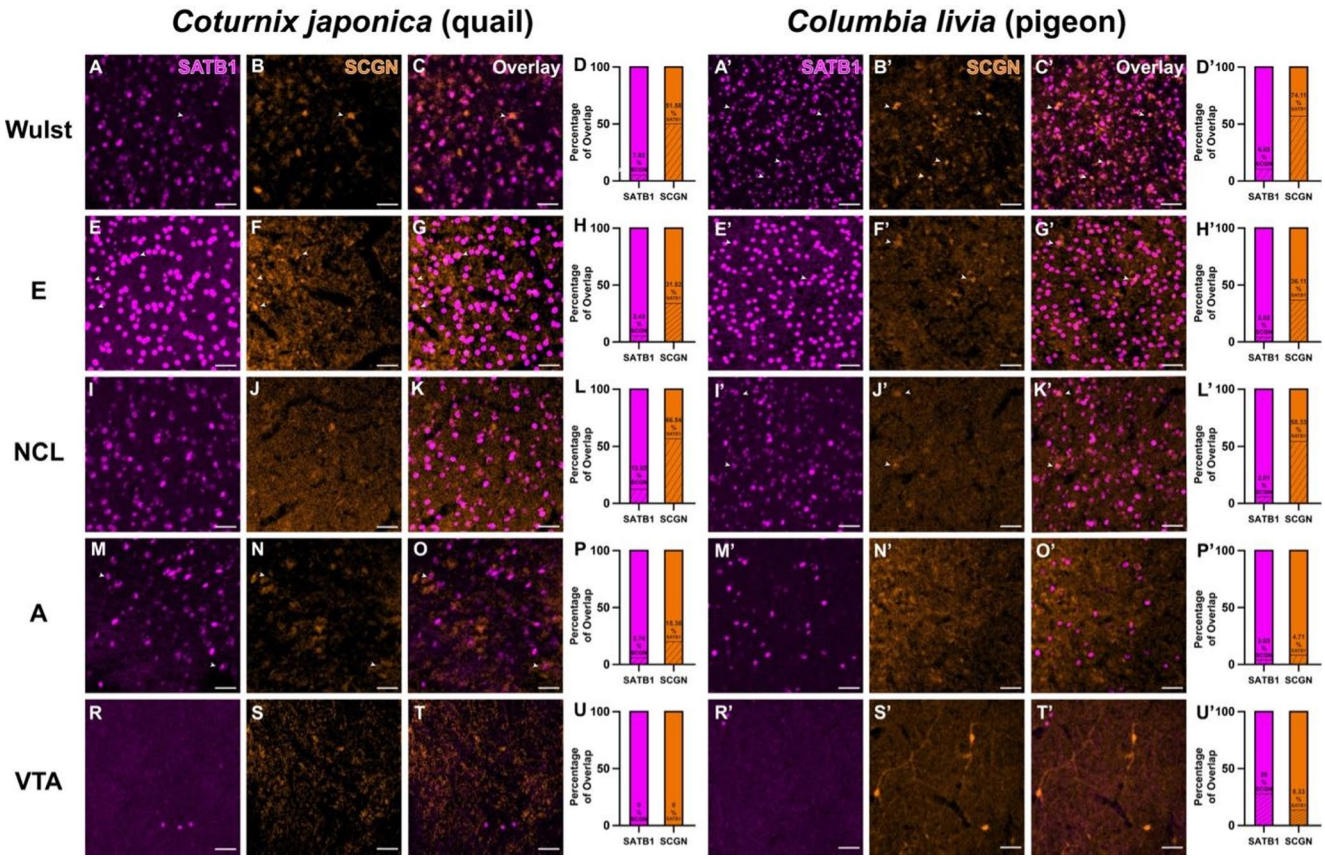



**Fig. 6** SCGN and SATB1 co-expression across pallial and midbrain regions in quail and pigeon. **A–U** Confocal images from quail showing SATB1 (**A**, **E**, **I**, **M**, **R**; magenta), SCGN (**B**, **F**, **J**, **N**, **S**; orange), and merged channels (**C**, **G**, **K**, **O**, **T**), together with stacked bar graphs showing marker co-expression (**D**, **H**, **L**, **P**, **U**). In each graph, the left bar indicates the proportion of SATB1 + cells co-expressing SCGN, and the right bar indicates the proportion of SCGN+ cells co-expressing SATB1. **A'–U'** Corresponding confocal images and bar graphs from pigeon. Arrowheads indicate representative double-labeled (SATB1+/SCGN+) neurons. A 1-pixel median filter was applied to all confocal images for noise reduction. Rows from top to bottom show the Wulst, entopallium (E), nidopallium caudolaterale (NCL), arcopallium (A), and ventral tegmental area (VTA). Scale bars: 50 μm

may reflect underlying differences in the inhibitory microcircuit organization of this higher-order associative area.

The arcopallium proper exhibited a distinct subregional gradient of SATB1 expression (Fig. 1E). Based on the topographic position of labeled neurons relative to the parcellation of the pigeon arcopallium/amygdala complex (Herold et al. 2018), the dorsal aspect of the arcopallium showed the highest density of immunopositive neurons, forming a well labeled domain. Intermediate levels of labeling were observed in the central arcopallial territory, while the ventral portion contained comparatively fewer SATB1 positive cells, resulting in a dorsal to ventral gradient of decreasing expression (Fig. 1E). This graded pattern may correspond to the distinct premotor and limbic compartments identified within the pigeon arcopallium (Herold et al. 2018; Zeier and Karten 1971).

The medial striatum (MSt) lacked SATB1 immunoreactivity, appearing as a large, conspicuously unlabeled territory within the ventral telencephalon, consistent with the pattern observed in quail (Fig. 1D). The absence of labeling in this subpallial region provided a useful internal landmark for delineating the pallial/subpallial boundary. We did not examine the diagonal band nuclei, which exhibit prominent SATB1 expression in mammals (Huang et al. 2011), and may therefore represent an informative subpallial population. At midbrain levels, the pigeon tectum showed notably lower SATB1 expression compared to the prominent and intense tectal labeling observed in quail (Fig. 1F). Similarly, VTA displayed only modest immunoreactivity with scattered SATB1 + somata (Fig. 1F, G), whose sparse distribution contrasted with the moderate VTA labeling observed in quail. This difference represents an additional axis of interspecific divergence and suggests that SATB1's regulatory role in midbrain circuits may vary between these columbiform and galliform species.

## GABA and SATB1 co-expression across pallial and midbrain regions

We performed SATB1/GABA double immunofluorescence to determine the proportion of avian SATB1+cells that belong to the GABAergic population across the five regions examined (Fig. 2). Across most pallial regions, only a minority of SATB1+neurons co-expressed GABA. In the quail Wulst, GABA+ cells averaged 24.00 (*SD*=7.35) and SATB1+cells averaged 136.75 (*SD*=45.06). While 18.69% of GABA+ cells co-expressed SATB1, only 4.25% of SATB1+cells co-expressed GABA (Fig. 2D; Table 2). A comparable pattern was observed in the pigeon Wulst, where GABA+ cells averaged 30.50 (*SD*=7.42) and SATB1+cells averaged 99.25 (*SD*=16.46), with 23.39% of GABA+ cells co-expressing SATB1 and 9.99% of SATB1+cells co-expressing GABA (Fig. 2D').

In the entopallium, the proportion of SATB1+cells that were GABAergic was similarly low in both species. In quail, GABA+ cells averaged 43.25 (*SD*=15.33) and SATB1+cells averaged 172.50 (*SD*=10.02). In this region 17.69% of GABA+ cells co-expressed SATB1 and 5.14% of SATB1+cells co-expressed GABA (Fig. 2H). In pigeon, GABA+ cells averaged 61.00 (*SD*=7.62) and SATB1+cells averaged 164.25 (*SD*=26.26), with 13.23% of GABA+ cells co-expressing SATB1 and 5.48% of SATB1+cells co-expressing GABA (Fig. 2H').

In the quail NCL, GABA+ cells averaged 48.75 (*SD*=19.87) and SATB1+cells averaged 76.25 (*SD*=34.50); and 37.21% of GABA+ cells co-expressed SATB1, while 10.39% of SATB1+cells co-expressed GABA (Fig. 2L). In pigeon, GABA+ cells averaged 36.75 (*SD*=4.50) and SATB1+cells averaged 123.00 (*SD*=14.94), with 28.04% of GABA+ cells co-expressing SATB1 and 8.79% of SATB1+cells co-expressing GABA (Fig. 2L').

In the arcopallium, the proportion of SATB1+cells co-expressing GABA was higher in quail than in pigeon. In quail, GABA+ cells averaged 60.50 (*SD*=12.23) and SATB1+cells averaged 40.75 (*SD*=34.58). Here, 11.62% of GABA+ cells co-expressed SATB1 and 24.29% of SATB1+cells co-expressed GABA (Fig. 2P). In pigeon, GABA+cells averaged 58.00 (*SD*=14.67) and SATB1+cells averaged 91.50 (*SD*=28.73), with 28.11% of GABA+ cells co-expressing SATB1 and 10.72% of SATB1+cells co-expressing GABA (Fig. 2P').

GABA+ cells were relatively abundant in the VTA of both species while SATB1+cells were comparatively few. In quail, GABA+ cells averaged 46.50 (*SD*=14.75) and SATB1+cells averaged 17.25 (*SD*=7.50). Only 4.63% of GABA+ cells co-expressed SATB1 and 13.55% of SATB1+cells co-expressed GABA (Fig. 2U). In pigeon, GABA+ cells averaged 69.00 (*SD*=13.78) and SATB1+cells averaged 17.50 (*SD*=3.70), with 6.52% of GABA+ cells co-expressing SATB1 and 20.84% of SATB1+cells co-expressing GABA (Fig. 2U').

Together, these results indicate that only a minority of SATB1+neurons in the avian pallium and midbrain co-express GABA, ranging from approximately 4% to 25% across regions and species. The highest proportions were observed in the quail arcopallium and in the VTA of both species. These findings suggest that, unlike the predominantly interneuron-associated expression reported in the mammalian cortex, many SATB1+neurons in the avian brain are likely glutamatergic. At the same time, the presence of a GABAergic subset demonstrates that SATB1 is also expressed by inhibitory neurons, consistent with reports of SATB1 expression in both inhibitory and excitatory neuronal populations in mammals (Balamotis et al. 2012).

## PV and SATB1 co-expression across pallial and midbrain regions

PV and SATB1 immunoreactivity revealed partially overlapping expression patterns across the five brain regions examined in both *Coturnix japonica* and *Columba livia* (Fig. 3). SATB1+neurons were broadly distributed in pallial regions and were particularly dense in the Wulst and entopallium of both species. PV+ neurons, by contrast, were consistently fewer in number than SATB1+neurons across all regions, appearing as a scattered population interspersed among the more abundant SATB1+cells.

In the Wulst, SATB1+cells were abundant in both species. In quail, PV+ cells averaged 25.56 (*SD*=17.73) and SATB1+cells averaged 147.11 (*SD*=40.93); 50.98% of PV+ cells co-expressed SATB1, and 13.04% of SATB1+cells co-expressed PV (Fig. 3D). In pigeon, PV+ cells were sparser (*M*=10.56, *SD*=5.41) alongside similarly abundant SATB1+cells (*M*=124.22, *SD*=44.16). Only 18.80% of PV+ cells co-expressed SATB1, and just 1.50% of SATB1+cells co-expressed PV (Fig. 3D'). Both overlap calculations were therefore markedly higher in quail than in pigeon.

In the entopallium, SATB1 expression was prominent in both species. In quail, PV+ cells averaged 15.00 (*SD*=11.90) and SATB1+cells averaged 105.00 (*SD*=24.92); 45.53% of PV+ cells co-expressed SATB1, and 11.69% of all SATB1+cells co-expressed PV (Fig. 3H). In pigeon, PV+ cells averaged 6.14 (*SD*=4.74) and SATB1+cells averaged 132.71 (*SD*=27.72). While 14.50% of PV+ cells showed SATB1 immunofluorescence, only 1.93% of SATB1+cells co-expressed PV (Fig. 3H'). The large standard deviations indicate considerable section-to-section variability, but the species difference in both overlap directions was nonetheless pronounced.

In the NCL, both PV+and SATB1+cell densities were moderate. In quail, PV+ cells averaged 4.25 (*SD*=2.96) and SATB1+cells averaged 62.38 (*SD*=20.47), with 37.69% of PV+ cells co-expressing SATB1, and 3.03% of SATB1+cells containing PV (Fig. 3L). Pigeon NCL also had a limited number of PV+ cells on average (*M*=8.33, *SD*=6.30), 10.31% of which co-expressed SATB1. SATB1+cells in the pigeon NCL (*M*=43.78, *SD*=27.48) were lower than in quail, consistent with qualitatively reduced SATB1 immunoreactivity in this region. Only a fraction of these (4.48%) were immunopositive for PV (Fig. 3L').

A notable species difference also emerged in the arcopallium. In quail, PV+ cells were sparse (*M*=3.67, *SD*=2.12) and SATB1+cells were moderately abundant (*M*=51.33, *SD*=28.55). About half (51.85%) of arcopallial PV+ cells co-expressed SATB1, while 7.86% of all SATB1+cells contained PV (Fig. 3P). In contrast, pigeon arcopallial PV+ cells (*M*=9.00, *SD*=3.74) and SATB1+cells (*M*=57.06, *SD*=15.74) showed only 7.07% of PV+ cells co-expressing SATB1, and 1.02% of SATB1+cells co-expressing PV (Fig. 3P'), indicating that the two populations were almost entirely separate, unlike quail arcopallium.

In the VTA, both PV and SATB1 expression was relatively low in both species. In quail, PV+ cells averaged 10.22 (*SD*=8.57) and SATB1+cells averaged 21.33 (*SD*=10.45). Only 4.74% of PV+ cells co-expressed SATB1, and 1.83% of SATB1+cells co-expressed PV (Fig. 3U). In pigeon, PV+ cells (*M*=9.50, *SD*=4.87) and SATB1+cells (*M*=13.88, *SD*=6.01) showed slightly higher overlap in both directions: 8.16% of PV+ cells co-expressed SATB1, and 6.05% of SATB1+cells co-expressed PV (Fig. 3U'). PV/SATB1 co-expression in the VTA was therefore minimal in both species.

Together, these results demonstrate that PV and SATB1 label largely distinct neuronal populations across most brain regions in both quail and pigeon, but with consistently higher co-expression in quail across all pallial regions examined. Across regions, the proportion of SATB1+cells co-expressing PV was always lower than the proportion of PV+ cells co-expressing SATB1, reflecting that SATB1+cells substantially outnumbered PV+ cells in the pallium and PV+ neurons therefore constituted only a small subset of the broader SATB1+population. SATB1 expression was highest in the Wulst and entopallium, whereas PV+ cell counts remained low across regions in both species. The arcopallium showed the most pronounced species divergence: in quail, the majority of PV+ neurons co-expressed SATB1, whereas in pigeon co-expression was nearly absent in both directions. The Wulst and entopallium of quail also showed substantially higher overlap than their pigeon counterparts, while the NCL and VTA exhibited modest to minimal co-expression in both species. Overall, these findings reveal region- and species-specific patterns in the neurochemical organization of PV+and SATB1+populations in the avian brain, with the arcopallium emerging as the main site of divergence.

## CR and SATB1 co-expression across pallial and midbrain regions

Double immunohistochemistry for CR and SATB1 revealed distinct but partially overlapping expression patterns in both avian species (Fig. 4). In the quail Wulst, SATB1+cells (*M*=131.88, *SD*=10.92) outnumbered CR+ cells (*M*=19.38, *SD*=7.01) with 32.60% of CR+ cells co-expressing SATB1, and 5.84% of SATB1+cells co-expressing CR (Fig. 4D). In pigeon, the Wulst contained markedly more CR+ cells (*M*=81.50, *SD*=32.14) alongside abundant SATB1+cells (*M*=135.36, *SD*=55.22). While 34.17% of CR+ cells co-expressed SATB1, a substantially higher proportion of SATB1+cells (43.95%) as compared to quail Wulst co-expressed CR (Fig. 4D'). The proportion of CR+ cells co-expressing SATB1 was therefore comparable between species, while the proportion of SATB1+cells co-expressing CR was nearly an order of magnitude higher in pigeon, reflecting the much greater density of CR+ neurons in the pigeon Wulst.

In the quail entopallium, CR+ cells averaged 12.25 (*SD*=11.99) and SATB1+cells averaged 118.38 (*SD*=48.61). A good proportion of CR+ cells (40.32%) co-expressed SATB1, while only 3.67% of all SATB1+cells co-expressed CR (Fig. 4H). There were fewer CR+ cells in the pigeon entopallium (*M*=14.71, *SD*=14.92) together with more abundant SATB1+cells (*M*=156.48 *SD*=41.62). Similar to quails, 36.97% of CR+ cells co-expressed SATB1, and 7.60% of SATB1+cells co-expressed CR (Fig. 4H').

In the NCL of quail, CR+ cells averaged 19.40 (*SD*=10.78) and SATB1+cells averaged 65.20 (*SD*=32.71). About half of CR+ cells (54.00%) co-expressed SATB1, and 7.65% of SATB1+cells co-expressed CR (Fig. 4L). The pigeon NCL exhibited slightly fewer CR+ cells (M=16.57, *SD*=9.02) and similar SATB1+cell counts (*M*=59.86, *SD*=53.99); 36.09% of CR+ cells co-expressed SATB1, and 11.13% of SATB1+cells co-expressed CR (Fig. 4L'). Quail NCL therefore showed a substantially higher proportion of CR+ cells co-expressing SATB1 than pigeon, while the proportion of SATB1+cells co-expressing CR was slightly higher in pigeon.

In the arcopallium, a striking interspecific difference in CR/SATB1 co-expression was observed. In quail, CR+ cells (*M*=17.50, *SD*=14.35) and SATB1+cells (*M*=57.55, *SD*=33.84) showed 68.56% of CR+ cells co-expressing SATB1, and 8.54% of SATB1+cells co-expressing CR (Fig. 4P), indicating that the majority of arcopallial CR+

neurons also expressed SATB1. In pigeon, CR+ cells were similarly numerous ($M$=18.71, $SD$=12.65) alongside comparable SATB1+counts ($M$=58.43, $SD$=44.64). Yet, 32.49% of CR+ cells co-expressed SATB1, and 15.36% of SATB1+cells co-expressed CR (Fig. 4P'). The proportion of CR+ cells co-expressing SATB1 was approximately half that observed in quail, whereas the proportion of SATB1+cells co-expressing CR was nearly twofold higher in pigeon.

In the VTA, CR+ cells were present at moderate densities while SATB1 expression was lower. In quail, CR+ cells averaged 14.29 ($SD$=7.39) and SATB1+cells averaged 9.57 ($SD$=4.93). Co-expression analysis showed 14.24% of CR+ cells containing SATB1, and 17.92% of SATB1+cells co-expressing CR (Fig. 4U). In pigeon, there were fewer CR+ cells ($M$=8.00, $SD$=2.65) and SATB1+cells ($M$=7.00, $SD$=7.00) on average, and only 6.06% of CR+ cells co-expressed SATB1, while 4.44% of SATB1+cells were immunopositive for CR (Fig. 4U').

These results indicate that CR and SATB1 label partially overlapping neuronal populations, with the extent of co-expression varying markedly across regions and species. The arcopallium and NCL showed pronounced interspecific differences in the proportion of CR+ cells co-expressing SATB1. In both regions, quail exhibited substantially higher proportions than pigeon, with the arcopallium reaching 68.56% in quail compared to 32.49% in pigeon. The pigeon Wulst was distinguished by an unusually high proportion of SATB1+cells co-expressing CR (43.95%), driven by the markedly greater density of CR+ neurons in this region. The VTA showed minimal co-expression in both species. Overall, these findings reveal both region- and species-specific differences in the neurochemical organization of CR+and CR+/SATB1+populations, with the arcopallium, NCL, and Wulst representing the most divergent regions between quail and pigeon.

## CB and SATB1 co-expression across pallial and midbrain regions

Calbindin-immunopositive neurons showed greater variability in density across regions and species (Fig. 5). In the quail Wulst, CB+ cells averaged 16.71 ($SD$=12.62) and SATB1+cells averaged 146.43 ($SD$=55.18). Several CB+ cells (43.39%) co-expressed SATB1, and a minority of SATB1+cells (4.39%) contained CB (Fig. 5D). In pigeon, CB+ cells were sparser ($M$=9.20, $SD$=4.85) alongside similarly abundant SATB1+cells ($M$=143.30, $SD$=49.50). Yet, they showed similar levels of co-expression: 32.79% of CB+ cells contained SATB1, and 3.72% of SATB1+cells were immunopositive for CB (Fig. 5D'). Both species therefore exhibited moderate proportions of CB+ cells co-expressing SATB1, whereas the proportion of SATB1+cells co-expressing CB in the Wulst was low in both species.

In the entopallium, CB+ cells were comparatively sparse. In quail, they averaged 21.43 ($SD$=17.63) while SATB1+cells averaged 120.29 ($SD$=52.18). About a third of CB+ cells (34.87%) co-expressed SATB1, and 9.45% of SATB1+cells co-expressed CB (Fig. 5H). In pigeon, they were even fewer CB+ cells ($M$=6.25, $SD$=3.01); yet 36.07% of these co-expressed SATB1. SATB1+cells in pigeon entopallium averaged 169.88 ($SD$=40.55) and only 1.05% of them were immunopositive for CB (Fig. 5H'). In short, the proportions of CB+ cells co-expressing SATB1 were comparable between species, while quail showed a substantially higher proportion of SATB1+cells co-expressing CB, reflecting the much greater density of CB+ neurons in the quail entopallium.

In the NCL, both species showed moderate CB+ cell counts. In quail, CB+ cells averaged 33.71 ($SD$=20.77) and SATB1+cells averaged 71.71 ($SD$=54.07); 29.58% of CB+ cells co-expressed SATB1, and 13.61% of SATB1+cells co-expressed CB (Fig. 5L). In pigeon, CB+ cells averaged 36.88 ($SD$=19.40) and SATB1+cells averaged 62.70 ($SD$=55.67). Similar to quail co-expression rates, 31.07% of CB+ cells were SATB1-immunopositive, and 13.53% of all SATB1+cells co-expressed CB (Fig. 5L'). Unlike the PV counts, CB+ cell numbers in the pigeon NCL were comparable to those in quail, and the proportions of CB+ cells co-expressing SATB1 and SATB1+cells co-expressing CB were nearly identical between the two species.

Both avian species exhibited moderate CB+ cell populations in the arcopallium, with substantial interspecific differences. In quail, 22.68% of CB+ cells ($M$=19.50, $SD$=18.96) co-expressed SATB1, and 6.77% of SATB1+cells ($M$=61.33, $SD$=46.82) co-expressed CB (Fig. 5P). The pigeon arcopallium exhibited similar levels of CB+ ($M$=14.17, $SD$=11.02) and SATB1+cells ($M$=64.17, $SD$=19.49). However, a larger proportion of CB+ cells (45.79%) co-expressed SATB1, while 10.68% of SATB1+cells contained CB (Fig. 5P').

Calbindin expression was limited in the VTA of both species. CB+ cells averaged 13.00 ($SD$=14.79) and SATB1+cells averaged 15.83 ($SD$=12.38) in the quail VTA with 14.75% of CB+ cells co-expressing SATB1, and 13.00% of SATB1+cells co-expressing CB (Fig. 5U). In pigeon, only 2.40% of VTA CB+ cells ($M$=9.29, $SD$=2.75) co-expressed SATB1, and 5.16% of SATB1+cells ($M$=6.71, $SD$=3.77) co-expressed CB (Fig. 5U').

In conclusion, CB+ cell counts were generally low to moderate across regions in both species. The arcopallium stood out as the primary site of interspecific difference, with pigeon showing approximately twice the proportion of CB+ cells co-expressing SATB1 compared to quail (45.79% vs.

22.68%), along with a higher proportion of SATB1 + cells co-expressing CB. In contrast, the Wulst, entopallium, and NCL exhibited moderate and broadly comparable levels of CB+ cells co-expressing SATB1 across species. The proportion of SATB1 + cells co-expressing CB remained low in most regions, consistent with the relative scarcity of CB+ cells compared to SATB1 + cells. The VTA showed minimal overlap in both species. Overall, these findings identify the arcopallium as a key locus of interspecific divergence between quail and pigeon, notably in the opposite direction to the PV/SATB1 and CR/SATB1 patterns, in which quail displayed higher arcopallial co-expression.

### SCGN and SATB1 co-expression across pallial and midbrain regions

SCGN-immunopositive cells were sparse in every region examined in both species, but a strikingly high proportion of them co-expressed SATB1. In the quail Wulst, SCGN+ cells averaged 19.50 (*SD* = 0.71) and SATB1 + cells averaged 138.50 (*SD* = 38.89); 51.58% of SCGN+ cells co-expressed SATB1, while 7.82% of SATB1 + cells co-expressed SCGN (Fig. 6D). The pigeon Wulst contained a comparable number of SCGN+ cells (*M* = 22.00, *SD* = 8.49) alongside a substantially larger SATB1 + population (*M* = 259.50, *SD* = 3.54). Here 74.11% of SCGN+ cells co-expressed SATB1, the highest proportion recorded for any marker in any region of either species, whereas only 6.53% of SATB1 + cells contained SCGN (Fig. 6D').

In the entopallium, SCGN+ cells were fewer in both species. In quail, SCGN+ cells averaged 7.00 (*SD* = 5.66) and SATB1 + cells averaged 127.00 (*SD* = 24.04), with 31.82% of SCGN+ cells co-expressing SATB1 and 2.43% of SATB1 + cells co-expressing SCGN (Fig. 6H). In pigeon, SCGN+ cells averaged 10.00 (*SD* = 11.31) and SATB1 + cells averaged 115.50 (*SD* = 23.33); 36.11% of SCGN+ cells co-expressed SATB1 and 2.02% of SATB1 + cells co-expressed SCGN (Fig. 6H'). The two species were therefore closely comparable in the entopallium in both directions of overlap, although the section-to-section variability was considerable in quail.

The NCL showed the highest proportion of SATB1 + cells co-expressing SCGN of any region examined. In quail, SCGN+ cells averaged 20.50 (*SD* = 7.78) and SATB1 + cells averaged 111.00 (*SD* = 2.83), with 66.54% of SCGN+ cells co-expressing SATB1 and 12.54% of SATB1 + cells co-expressing SCGN (Fig. 6L). The pigeon NCL contained markedly fewer SCGN+ cells (*M* = 5.00, *SD* = 1.41) alongside more abundant SATB1 + cells (*M* = 146.00, *SD* = 15.56); 58.33% of SCGN+ cells co-expressed SATB1, but only 2.01% of SATB1 + cells co-expressed SCGN (Fig. 6L'). The proportion of SCGN+ cells engaging SATB1 was therefore similar across species, while the reciprocal measure differed by roughly sixfold, reflecting the sparser SCGN+ population and larger SATB1 + population in pigeon.

In contrast to every other region, the arcopallium showed low SCGN/SATB1 overlap in both species. In quail, SCGN+ cells averaged 15.00 (*SD* = 2.83) and SATB1 + cells averaged 50.50 (*SD* = 31.82), with 15.38% of SCGN+ cells co-expressing SATB1 and 2.74% of SATB1 + cells co-expressing SCGN (Fig. 6P). In pigeon, SCGN+ cells averaged 10.00 (*SD* = 7.07) and SATB1 + cells averaged 33.50 (*SD* = 12.02); only 3.33% of SCGN+ cells co-expressed SATB1 and 2.00% of SATB1 + cells co-expressed SCGN (Fig. 6P'). Unlike PV, CR, and CB, SCGN therefore did not distinguish the quail from the pigeon arcopallium; instead, both species showed the lowest overlap of any pallial region.

In the midbrain, SCGN labeling was observed in both species, whereas SATB1 expression was relatively sparse, with little overlap between the two markers. In the quail VTA, SCGN+ cells averaged 5.50 (*SD* = 3.54) and SATB1 + cells averaged 11.00 (*SD* = 0.00); no double-labeled cells were detected (Fig. 6U). SCGN+ somata and processes were also evident in the pigeon VTA (*M* = 6.50, *SD* = 0.71), but SATB1 + cells were nearly absent from this region in the present series (*M* = 2.00, *SD* = 0.00). Despite the low number of SATB1 + cells, overlap between the markers was detected in the pigeon VTA, with double-labeled cells accounting for 8.33% of SCGN+ cells and 25.00% of SATB1 + cells (Fig. 6U′).

Taken together, these observations identify SCGN as the calcium-binding protein whose expression is most consistently associated with SATB1 in the avian pallium. In the Wulst and NCL, roughly half to three-quarters of SCGN+ cells co-expressed SATB1 in both species, exceeding the corresponding proportions for PV, CR, and CB in nearly every comparison. Because SCGN+ cells were numerically sparse, however, they accounted for only a small fraction of the total SATB1 + population, ranging from approximately 2% to 13% across pallial regions. The arcopallium and VTA departed from this pattern, showing minimal overlap in both species.

## Discussion

This study provides a systematic characterization of SATB1 expression and its co-localization with GABA and multiple calcium-binding proteins across pallial and midbrain regions in two avian species. The selected regions represent functionally distinct domains of the avian brain. The Wulst, the primary somatosensory and visual recipient zone of the thalamofugal pathway, is considered a homologue of the mammalian primary sensory cortex (Jarvis et al. 2005;

Medina and Reiner 2000). The entopallium serves as the telencephalic target of the tectofugal visual pathway and plays a key role in visual object processing (Husband and Shimizu 1999; Stacho et al. 2016). The NCL is a higher-order associative region regarded as a functional analogue of the mammalian prefrontal cortex. This functional analogy rests on shared connectivity, dense dopaminergic innervation, and involvement in executive functions rather than on cytoarchitectonic similarity, as the NCL has a nuclear rather than a laminar organization (Güntürkün 2005; Herold et al. 2011). The arcopallium is a premotor and limbic output structure, partially comparable to the mammalian amygdala and motor cortical areas (Jarvis et al. 2005; Reiner et al. 2004). To extend the analysis beyond the pallium, we included midbrain regions, quantifying SATB1 expression in the VTA, a key dopaminergic nucleus (von Eugen et al. 2020), and noting a striking interspecific difference in the optic tectum, which showed robust SATB1 labeling in quail but comparatively low expression in pigeon.

SATB1 delineated several brain regions with considerable precision, including the entopallium, IHA, field L2, and arcopallium. The NCL was distinguishable from neighboring regions at some rostrocaudal levels but not others, indicating a level-dependent delineation by SATB1. Co-localization analysis revealed that it marks largely distinct neuronal populations relative to each calcium-binding protein, with the degree of co-expression varying across regions and between species. The arcopallium emerged as the most divergent region: in quail, the majority of PV + and CR+ neurons co-expressed SATB1, whereas in pigeon CB+ neurons showed the highest SATB1 overlap. Quail also showed substantially higher PV/SATB1 co-expression than pigeon throughout the Wulst and entopallium, while CB and CR co-expression patterns in these sensory regions were broadly comparable between the two avian species. The NCL and VTA showed generally low overlap. These findings establish SATB1 as a regional marker in the avian brain and reveal species-specific patterns in its relationship with classical interneuron markers that both parallel and diverge from the organizational principles described in the mammalian cortex. Notably, co-labeling with GABA revealed that only a minor fraction of SATB1 + neurons in the avian pallium and midbrain are GABAergic, indicating that, unlike the predominantly interneuron-associated expression reported in the mammalian cortex, a substantial proportion of avian SATB1 + cells are likely glutamatergic.

## SATB1 as a chemoarchitectonic marker in the avian pallium

A consistent finding across both species was the capacity of SATB1 to sharply delineate specific pallial territories. In the entopallium, dense SATB1 labeling produced a clearly demarcated domain that stood out against the surrounding nidopallium and mesopallium, in both quail and pigeon, confirming its utility as a boundary marker for this visual thalamorecipient structure. This is consistent with the known enrichment of specific transcription factors in avian sensory thalamorecipient zones (Dugas-Ford et al. 2012; Jarvis et al. 2013), and extends previous immunohistochemical work showing differential PV and CB distribution in pigeon entopallium (Belekhova et al. 2018). SATB1 expression in the IHA clearly separated this thalamorecipient layer from both the overlying HA and the MD in both species. The distinction between the deepest Wulst layers and the MD has long been a source of confusion in the literature, as some earlier studies did not differentiate these structures (Jarvis et al. 2013). The sharp SATB1-defined boundary observed here complements earlier work using combinations of CB, CR, GABA and nNOS to distinguish Wulst subdivisions in chicken (Suárez et al. 2006), and provides an additional molecular criterion for resolving this boundary.

In pigeon, SATB1 additionally delineated the boundary between the NCM and MD, showing a sharp molecular transition that was more clearly defined than in conventional Nissl-based cytoarchitectonics. Moreover, intense SATB1 labeling highlighted Field L2, a structure that can be difficult to identify using conventional histological stains (Reiner et al. 2004). The capacity of SATB1 to delineate multiple thalamorecipient domains across sensory modalities, visual in the entopallium and Wulst and auditory in Field L2, suggests that its expression may represent a shared feature of primary sensory input zones in the avian pallium, potentially reflecting a conserved transcriptional identity.

A second organizational feature highlighted by SATB1 was the presence of graded expression patterns within nominally uniform structures. In the quail caudal nidopallium, SATB1 immunoreactivity formed a clear medial-to-lateral gradient, with the NCM essentially devoid of labeling, the nidopallium caudale island fields (NClF) showing intermediate expression, and the NCL densely labeled. This gradient parallels the functional subdivision of the caudal nidopallium into auditory associative (NCM) and executive associative (NCL) compartments, and suggests that SATB1 expression tracks the transition from sensory associative to higher-order associative processing along the mediolateral axis. Another graded pattern was observed in the pigeon arcopallium, where SATB1 immunoreactivity decreased along a dorsoventral axis, with the arcopallium dorsale showing the highest density of labeled neurons, the arcopallium intermedium an intermediate density, and the arcopallium ventrale the lowest. The pigeon arcopallium proper contains distinct premotor compartments (Herold et al. 2018; Zeier and Karten 1971), within which the dorsoventral

SATB1 gradient described here suggests an additional layer of organization, potentially reflecting compartment-specific interneuron patterning. Together, these graded patterns indicate that SATB1 captures not only categorical boundaries between pallial fields but also continuous organizational features within them.

The most striking interspecific difference in SATB1 distribution was observed in the NCL. In quail, the NCL was one of the most densely SATB1-labeled pallial regions, and represented the lateral extreme of the medial-to-lateral nidopallial gradient described above; whereas in pigeon it showed qualitatively lower immunoreactivity with a more dispersed population of labeled cells. In the mammalian prefrontal cortex, SATB1 is expressed in specific types of interneuron that contribute to local inhibitory microcircuits (Close et al. 2012; Denaxa et al. 2012). The variable SATB1 expression in the avian NCL raises the question of whether interspecific differences in SATB1 + cell density contribute to variation in the inhibitory architecture of this higher-order associative region, which may relate to the behavioral and cognitive differences between galliforms and columbiforms.

## SATB1 expression in the midbrain

Beyond the pallium, SATB1 labeled the optic tectum and VTA in both species, though with notable interspecific differences. In quail, the tectum exhibited some of the strongest SATB1 labeling observed in the entire brain, whereas in pigeon tectal labeling was markedly reduced. The VTA showed moderate SATB1 expression in quail and only modest labeling in pigeon. Recent work in zebra finches and Japanese quails has demonstrated that CB, CR, and PV are differentially distributed across VTA and substantia nigra subdivisions, and co-localize with tyrosine hydroxylase in subtype-specific patterns (Albayrak et al. 2026; Mitra et al. 2022), suggesting substantial neurochemical heterogeneity of the avian midbrain dopaminergic neurons. The presence of SATB1 in the avian VTA, albeit at low levels, raises the possibility that this transcription factor contributes to the molecular specification of midbrain neuronal subtypes in birds, a hypothesis that warrants further investigation with dopaminergic co-labeling.

## Avian interspecific differences in SATB1/calcium-binding protein co-expression

The co-localization analyses revealed that SATB1 and the canonical calcium-binding proteins mark largely non-overlapping neuronal populations across most regions in both species, with region- and species-specific exceptions, and with SCGN representing a systematic departure from this pattern. The general finding for PV, CR, and CB is consistent with the mammalian literature, where SATB1 is expressed in subsets of PV+ interneurons while remaining absent from CGE-derived populations that include CR+ neurons (Close et al. 2012; Denaxa et al. 2012).

The arcopallium exhibited the greatest interspecific divergence across all three canonical markers. In quail, the majority of PV + and CR+ neurons co-expressed SATB1, whereas CB/SATB1 overlap was more modest. In pigeon this pattern was reversed, with low PV/SATB1 and CR/SATB1 overlap but the highest CB/SATB1 co-expression observed in any region or species. This bidirectional divergence is striking and suggests that the arcopallium of quail and pigeon, despite being homologous structures, differ fundamentally in the neurochemical identity of their SATB1-expressing neuronal populations. The dorsoventral SATB1 gradient observed in pigeon arcopallium (AD > AI > AV) raises the additional possibility that the high CB/SATB1 co-expression in this region may be concentrated within specific arcopallial subdivisions rather than uniformly distributed. In the mammalian amygdala, to which the avian arcopallium is partially comparable (Jarvis et al. 2005; Reiner et al. 2004), PV+, CB+, and CR+ interneurons occupy distinct subregions with different co-expression profiles (Mascagni and McDonald 2003; Pitkänen and Kemppainen 2002). The interspecific differences observed here may therefore reflect lineage-specific modifications in inhibitory microcircuit organization within an arcopallial territory that subserves distinct functional roles in galliforms and columbiforms.

The Wulst and entopallium showed mixed patterns of conservation and divergence across markers. PV/SATB1 co-expression was substantially higher in quail than in pigeon in both the Wulst and entopallium, suggesting that PV+ neurons in primary sensory pallial regions engage SATB1-dependent transcriptional programs to a greater extent in quail. By contrast, CB/SATB1 overlap was moderate and broadly similar across species in these structures, and CR/SATB1 co-expression was likewise comparable. The pigeon Wulst was nonetheless distinguished by a much higher absolute density of CR+ neurons than the quail Wulst, which produced a markedly elevated proportion of SATB1 + cells co-expressing CR.

SCGN showed a distinct relationship with SATB1 compared with the three canonical calcium-binding proteins. Across the Wulst and NCL, approximately half to three-quarters of SCGN+ cells co-expressed SATB1 in both quail and pigeon, representing the highest and most consistent interspecific overlap observed in this study. In mammals, SCGN labels a population of telencephalic neurons that is largely complementary to those expressing PV, CB, and CR (Alpár et al. 2012; Mulder et al. 2009), including cortical GABAergic interneurons of mixed ganglionic-eminence origin (Alzu'bi and Clowry 2020) and a topographically

segregated subset of striatal PV+ interneurons in rats and primates (Garas et al. 2016). Similarly, in birds, SCGN has been reported to characterize neuronal populations that complement the distribution of the canonical calcium-binding proteins in the telencephalon and midbrain of the domestic chick (Gáti et al. 2014), as well as GAD-expressing Lugaro-like interneurons in the pigeon cerebellum (Craciun et al. 2019). The consistent association between SCGN and SATB1 observed here suggests that the sparse avian SCGN+ population is preferentially recruited from the broader SATB1 + compartment. However, because SCGN+ cells represented only 2–13% of SATB1 + cells across pallial regions, a proportion comparable to the 4–25% of SATB1 + cells that were GABA-immunopositive, the SCGN+/SATB1 + population may represent a subset of the GABAergic minority within the broader SATB1 + compartment. Notably, the arcopallium, which showed the greatest interspecific divergence in PV, CR, and CB expression, exhibited uniformly low SCGN/SATB1 overlap in both species. This finding suggests that the pronounced interspecific divergence observed in the arcopallium is specific to particular calcium-binding protein populations rather than reflecting a broader species difference in the composition of SATB1 + neurons in this region.

The comparisons above should be interpreted with caution, as cell counts showed some section-to-section variability in both species (Table 2). Two additional limitations warrant consideration. First, GABA immunolabeling in aldehyde-fixed tissue without glutaraldehyde incompletely detects somatic GABA, making the reported proportion of GABAergic SATB1 + cells more likely an underestimate than an overestimate. Nevertheless, the magnitude of the effect, together with evidence for SATB1 expression in excitatory neurons of the mammalian neocortex (Balamotis et al. 2012), supports the presence of a substantial non-GABAergic SATB1 + population. Second, we did not directly co-label SATB1 with a glutamatergic marker; thus, assigning GABA-negative SATB1 + cells to a glutamatergic phenotype remains inferential, based on the predominance of either GABAergic or glutamatergic identities among avian pallial neurons (Colquitt et al. 2021; Zaremba et al. 2025). Direct confirmation using vesicular glutamate transporter labeling or *SLC17A6* in situ hybridization will be an important next step. Finally, the species differ in their behavioral specializations: pigeons are widely studied for visual categorization, spatial cognition, and associative learning, whereas quail have been studied more extensively in reproductive and appetitive conditioning. Whether the observed interspecific differences in SATB1/calcium-binding protein co-expression, particularly in the arcopallium, relate to these behavioral specializations remains speculative and will require targeted functional studies.

## SATB1 and interneuron lineage

In mammals, the developmental origin of cortical interneurons from the MGE versus the CGE establishes a fundamental organizational principle: PV + and SST+ interneurons arise primarily from the MGE and express SATB1 as part of a Nkx2.1-Lhx6-SATB1 transcriptional cascade, whereas CR + and VIP+ interneurons arise largely from the CGE and remain SATB1-negative (Butt et al. 2008; Close et al. 2012; Denaxa et al. 2012; Wonders and Anderson 2006). Calbindin occupies an intermediate position, being expressed in subsets of both MGE-derived SST+ neurons and certain CGE-derived populations, and therefore shows region-dependent co-localization with SATB1 (Fogarty et al. 2007; Xu et al. 2008).

The avian data reported here both align with and diverge from this framework. The substantial PV/SATB1 co-expression observed in quail sensory regions is broadly consistent with a mammalian-like pattern, in which a large fraction of PV+ neurons engages SATB1-dependent programs, although the markedly lower PV/SATB1 overlap in the corresponding pigeon regions suggests that this relationship is not uniformly conserved across birds. In contrast, the pronounced CR/SATB1 co-expression observed in several regions, most notably in the quail arcopallium and NCL, represents a clear departure from the mammalian model, where CR+ neurons are predominantly CGE-derived and typically lack SATB1. This discrepancy could reflect several possibilities. First, avian CR+ neurons may comprise both MGE- and CGE-equivalent lineages, with the SATB1-expressing fraction corresponding to MGE-derived cells that also express CR. Consistent with this, recent single-cell transcriptomic studies in songbirds and chickens indicate that avian pallial interneurons comprise both MGE- and CGE-like classes, but in proportions distinct from mammals, with MGE-like interneurons predominating and CGE-like neurons representing only a small fraction of the GABAergic population (Colquitt et al. 2021; Zaremba et al. 2025). If the CGE-like compartment is indeed reduced in birds, a larger proportion of CR+ neurons may belong to MGE-like lineages that express SATB1. Second, the transcriptional identity of avian CR+ neurons may have diverged, such that CR expression is not exclusively associated with CGE-derived identity. Third, SATB1 may exhibit a broader expression domain in birds than in its mammalian orthologue, encompassing both MGE-equivalent and non-MGE cell types (Huang et al. 2011).

A key constraint on these lineage-based interpretations is provided by our SATB1/GABA co-labeling data. Across regions, only a minority of SATB1 + cells co-expressed GABA, ranging from approximately 4% to 25%, with the highest proportions observed in the quail arcopallium and in

the VTA of both species. These findings indicate that a substantial proportion of avian SATB1 + neurons are not GABAergic and are therefore likely glutamatergic, consistent with the well-established expression of SATB1 in excitatory pyramidal neurons of the mammalian neocortex (Balamotis et al. 2012). This observation has two implications. First, it cautions against interpreting SATB1 as an exclusively interneuron-associated marker in birds. Although a GABAergic SATB1 + population is clearly present, a large fraction of SATB1 + neurons likely represents excitatory cells. Second, it provides a parsimonious explanation for the high levels of CR/SATB1 co-expression and, in some regions, CB/SATB1 co-expression that differ from the canonical mammalian interneuron pattern. Rather than reflecting an expanded population of MGE-derived CR+ interneurons, at least some of these double-labeled cells may be glutamatergic neurons that co-express CR or CB.

The CB/SATB1 co-expression pattern was more uniform across species and regions than the PV or CR patterns, with most pallial regions showing moderate overlap. The arcopallium was the principal exception, where pigeon showed substantially higher CB/SATB1 overlap (45.79%) than quail (22.68%). This relatively even CB/SATB1 distribution is broadly consistent with the mammalian pattern, in which CB is expressed by a substantial proportion of SATB1-positive SST+ interneurons (Close et al. 2012; Fogarty et al. 2007), although the elevated pigeon arcopallial overlap suggests lineage specific expansion of a CB/SATB1 double-immunopositive population in this region. It is also worth noting that in zebra finch HVC, interneurons can be immunopositive for one, two, or all three calcium-binding proteins simultaneously (Wild et al. 2005), a pattern of extensive co-expression that differs from the largely non-overlapping expression in the mammalian neocortex, further underscoring that rules governing calcium-binding protein expression in avian interneurons do not simply mirror the mammalian pattern.

## Cross-species conservation and divergence of SATB1 expression in vertebrates

SATB1 is widely expressed across prefrontal, somatosensory, and visual areas of the rodent neocortex, primarily in PV + and SST+ interneurons, while excluding specific interneuron types such as CGE-derived 5-HT3aR-expressing cells (Close et al. 2012; Denaxa et al. 2012; Huang et al. 2011). This selectivity supports its role as a molecular marker distinguishing interneuron classes of different developmental origin (Kepecs and Fishell 2014). In addition to the neocortex, SATB1 labels hippocampal PV + and SST+ interneurons but is absent from axo-axonic cells (Viney et al. 2013), and is also found in subsets of primate retinal ganglion cells (Nasir-Ahmad et al. 2021). In birds, SATB1 is broadly expressed across pallial regions, including proposed homologues of mammalian cortical and amygdaloid areas (Güntürkün 2005; Jarvis et al. 2005; Reiner et al. 2004), paralleling its widespread cortical distribution in mammals.

Within the rodent cortex, however, SATB1 + interneurons are distributed across functionally and architectonically distinct areas, including primary sensory isocortex, limbic mesocortex, and hippocampal allocortex, broadly following the proportions of MGE-derived interneuronal populations across the cortical sheet (Huang et al. 2011). Comparisons between birds and mammals should therefore take into account the specific cortical type involved, as the avian pallial regions examined here are not uniformly homologous to a single mammalian cortical area. Furthermore, our GABA co-labeling indicates that, unlike in the mammalian cortex, only a minor fraction of avian pallial SATB1 + cells are GABAergic, suggesting that the avian SATB1 + population is not predominantly interneuron-associated and includes a substantial putatively glutamatergic component. Hence, we observed moderate PV/SATB1 co-expression in avian sensory regions, partially recapitulating the mammalian pattern, but relatively high CR/SATB1 co-expression, which diverges from mammals.

Single-cell transcriptomic work in reptiles has shown that the major classes of cortical GABAergic interneurons, including MGE- and CGE-derived populations, are deeply conserved across amniotes (Tosches et al. 2018). This conservation implies that the avian interneuron classes labeled by SATB1 and the calcium-binding proteins examined here are most likely homologous to their mammalian counterparts, and the discussed interspecific differences reflect lineage-specific modifications of a shared ancestral program rather than independently evolved cell types.

Additional evidence comes from bony fishes, where SATB1 protein domains are highly conserved across sarcopterygian and actinopterygian lineages despite marked differences in expression patterns (Lozano et al. 2023). Pallial SATB1 expression was detected only in lungfish, the sole sarcopterygian examined, and was absent from the pallium of all actinopterygian species studied. In contrast, SATB1 expression was present in several midbrain regions of actinopterygians. This combination of molecular conservation and spatial divergence parallels our findings in birds, where SATB1 is expressed in the pallium of both quail and pigeon but exhibits species-specific regional distributions. Similar differences were observed in the midbrain, particularly in the optic tectum, where SATB1 labeling was strong and layer-specific in quail but markedly reduced in pigeon. Together, these comparisons are consistent with the possibility that pallial SATB1 expression represents an ancestral

sarcopterygian feature that has undergone lineage-specific diversification within tetrapods, whereas midbrain SATB1 expression may be more broadly conserved across bony vertebrates.

## Conclusion

This study yields three main conclusions. First, SATB1 serves as a useful chemoarchitectonic marker in the avian brain, sharply delineating sensory thalamorecipient regions such as the entopallium, IHA, and field L2, while also revealing organizational features within the caudal nidopallium and arcopallium that are not always apparent with conventional staining methods. Second, SATB1 and the calcium-binding proteins label largely distinct neuronal populations, with patterns of co-expression varying across regions and between species. Notably, PV/SATB1 co-expression in sensory pallial regions is higher in quail than in pigeon, CR/SATB1 co-expression is substantial in several regions and differs from the canonical mammalian pattern, and the arcopallium exhibits pronounced species differences, with PV and CR showing greater co-expression with SATB1 in quail and CB showing greater co-expression in pigeon. SCGN, in contrast, showed the highest and most species-consistent overlap with SATB1 of any calcium-binding protein examined. SATB1/GABA co-labeling revealed that only a minority of avian SATB1 + cells are GABAergic, indicating that, unlike the predominantly interneuron-associated expression reported in the mammalian cortex, many SATB1 + neurons in the avian brain are likely glutamatergic. Thus, SATB1 marks a mixed population of inhibitory and excitatory neurons rather than a purely interneuron-defined population.

Together, these findings expand the comparative framework for understanding vertebrate neuronal diversity, suggest that SATB1-associated neuronal programs reflect both evolutionary conservation and lineage-specific divergence in birds, and identify the arcopallium as a promising target for future studies examining the evolution of inhibitory circuit organization and its relationship to behavior and cognition.

**Author contributions** All authors contributed to study conception and design, data collection and analysis, and manuscript preparation.

**Funding** This research was supported by grants from the Scientific and Technological Research Council of Türkiye (Project Numbers: 123K557 and 123N516) to GU as well as SFB1372 Project-ID 395940726 and AVIAN MIND, ERC-2020-ADG, LS5, GA No. 101021354 to OG.

**Data availability** All data will be made available upon reasonable request.

## Declarations

**Competing interests** The authors declare no competing interests.

## References

Albayrak D, Gencturk S, Haselhuhn KB, Sevinc C, Güntürkün O, Behroozi M, Rook N, Unal G (2026) Dopaminergic Innervation of the Nidopallium Caudolaterale in the Japanese Quail. J Comp Neurol 534(4):e70154. https://doi.org/10.1002/CNE.70154

Alpár A, Attems J, Mulder J, Hökfelt T, Harkany T (2012) The renaissance of Ca2+-binding proteins in the nervous system: Secretagogin takes center stage. Cell Signal 24(2):378–387. https://doi.org/10.1016/j.cellsig.2011.09.028

Alzu'bi A, Clowry GJ (2020) Multiple origins of secretagogin expressing cortical GABAergic neuron precursors in the early human fetal telencephalon. Front Neuroanat 14:61. https://doi.org/10.3389/fnana.2020.00061

Amilhon B, Huh CYL, Manseau F, Ducharme G, Nichol H, Adamantidis A, Williams S (2015) Parvalbumin Interneurons of Hippocampus Tune Population Activity at Theta Frequency. Neuron 86(5):1277–1289. https://doi.org/10.1016/j.neuron.2015.05.027

Attems J, Preusser M, Grosinger-Quass M, Wagner L, Lintner F, Jellinger K (2008) Calcium-binding protein secretagogin-expressing neurones in the human hippocampus are largely resistant to neurodegeneration in Alzheimer's disease. Neuropathol Appl Neurobiol 34(1):23–32. https://doi.org/10.1111/j.1365-2990.2007.00854.x https://doi.org/10.1111/j.1365-2990.2007.00854.x

Balamotis MA, Tamberg N, Woo YJ, Li J, Davy B, Kohwi-Shigematsu T, Kohwi Y (2012) Satb1 Ablation Alters Temporal Expression of Immediate Early Genes and Reduces Dendritic Spine Density during Postnatal Brain Development. Mol Cell Biol 32(2):333. https://doi.org/10.1128/mcb.05917-11

Belekhova MG, Vasilyev DS, Kenigfest NB, Chudinova TV (2018) Calcium-Binding Proteins and Cytochrome Oxidase Activity in the Pigeon Entopallium: A Comparative Analysis of Interspecies Variability as Related to the Discussion on Avian Entopallium Homology. J Evol Biochem Physiol 2018 54(1):1. https://doi.org/10.1134/S0022093018010088

Bhagwandin A, Sherwood CC, Hof PR, Bertlesen MF, Alagaili AN, Mohammed OB, Bennett NC, Kaswera-Kyamakya C, Gilissen E, Manger PR (2024) Parvalbumin, calbindin, and calretinin immunostaining of 10 neural structures within the cerebellar cortex of 143 mammal species. Front Mammal Sci 3:1355791. https://doi.org/10.3389/fmamm.2024.1355791

Butt SJB, Sousa VH, Fuccillo MV, Hjerling-Leffler J, Miyoshi G, Kimura S, Fishell G (2008) The Requirement of Nkx2-1 in the Temporal Specification of Cortical Interneuron Subtypes. Neuron 59(5):722–732. https://doi.org/10.1016/j.neuron.2008.07.031

Close J, Xu H, García NDM, Batista-Brito R, Rossignol E, Rudy B, Fishell G (2012) Satb1 Is an Activity-Modulated Transcription Factor Required for the Terminal Differentiation and Connectivity of Medial Ganglionic Eminence-Derived Cortical Interneurons. J Neurosci 32(49):17690. https://doi.org/10.1523/JNEUROSCI.3583-12.2012

Colquitt BM, Merullo DP, Konopka G, Roberts TF, Brainard MS (2021) Cellular transcriptomics reveals evolutionary identities of songbird vocal circuits. Science 371(6530):eabd9704. https://doi.org/10.1126/science.abd9704

Craciun I, Gutierrez-Ibanez C, Chan ASM, Luksch H, Wylie DR (2019) Secretagogin immunoreactivity reveals Lugaro cells in the pigeon cerebellum. Cerebellum 18(3):544–555. https://doi.org/10.1007/s12311-019-01023-7

Denaxa M, Kalaitzidou M, Garefalaki A, Achimastou A, Lasrado R, Maes T, Pachnis V (2012) Maturation-Promoting Activity of SATB1 in MGE-Derived Cortical Interneurons. Cell Rep 2(5):1351. https://doi.org/10.1016/j.celrep.2012.10.003

Dugas-Ford J, Rowell JJ, Ragsdale CW (2012) Cell-type homologies and the origins of the neocortex. Proc Natl Acad Sci 109(42):16974–16979. https://doi.org/10.1073/PNAS.1204773109

Fogarty M, Grist M, Gelman D, Marín O, Pachnis V, Kessaris N (2007) Spatial genetic patterning of the embryonic neuroepithelium generates GABAergic interneuron diversity in the adult cortex. J Neuroscience: Official J Soc Neurosci 27(41):10935–10946. https://doi.org/10.1523/JNEUROSCI.1629-07.2007

Garas FN, Shah RS, Kormann E, Doig NM, Vinciati F, Nakamura KC, Dorst MC, Smith Y, Magill PJ, Sharott A (2016) Secretagogin expression delineates functionally-specialized populations of striatal parvalbumin-containing interneurons. eLife 5:e16088. https://doi.org/10.7554/eLife.16088

Gáti G, Lendvai D, Hökfelt T, Harkany T, Alpár A (2014) Revival of calcium-binding proteins for neuromorphology: Secretagogin typifies distinct cell populations in the avian brain. Brain Behav Evol 83(2):82–92. https://doi.org/10.1159/000357834

Gulyás AI, Hájos N, Freund TF (1996) Interneurons containing calretinin are specialized to control other interneurons in the rat hippocampus. J Neuroscience: Official J Soc Neurosci 16(10):3397–3411. https://doi.org/10.1523/jneurosci.16-10-03397.1996

Güntürkün O (2005) The avian 'prefrontal cortex' and cognition. Curr Opin Neurobiol 15(6):686–693. https://doi.org/10.1016/J.CONB.2005.10.003

Güntürkün O, Bugnyar T (2016) Cognition without Cortex. Trends Cogn Sci 20(4):291–303. https://doi.org/10.1016/j.tics.2016.02.001

Halpern BP, Karten HJ, Hodos W (1967) A stereotaxic atlas of the brain of the pigeon (Columba livia). Am J Psychol 81(2):289. https://doi.org/10.2307/1421283

Herold C, Palomero-Gallagher N, Hellmann B, Kröner S, Theiss C, Güntürkün O, Zilles K (2011) The receptor architecture of the pigeons' nidopallium caudolaterale: an avian analogue to the mammalian prefrontal cortex. Brain Struct Funct 216(3):239–254 https://doi.org/10.1007/s00429-011-0301-5

Herold C, Paulitschek C, Palomero-Gallagher N, Güntürkün O, Zilles K (2018) Transmitter receptors reveal segregation of the arcopallium/amygdala complex in pigeons (Columba livia). J Comp Neurol 526(3):439–466. https://doi.org/10.1002/CNE.24344

Hijazi S, Smit AB, van Kesteren RE (2023) Fast-spiking parvalbumin-positive interneurons in brain physiology and Alzheimer's disease. Mol Psychiatry 28(12):4954. https://doi.org/10.1038/s41380-023-02168-y

Hof PR, Glezer II, Condé F, Flagg RA, Rubin MB, Nimchinsky EA, Weisenhorn V, D. M (1999) Cellular distribution of the calcium-binding proteins parvalbumin, calbindin, and calretinin in the neocortex of mammals: Phylogenetic and developmental patterns. J Chem Neuroanat 16(2):77–116. https://doi.org/10.1016/S0891-0618(98)00065-9

Hu JS, Vogt D, Sandberg M, Rubenstein JL (2017) Cortical interneuron development: a tale of time and space. Development 144(21):3867–3878. https://doi.org/10.1242/dev.132852

Huang Y, Zhang L, Song NN, Hu ZL, Chen JY, Ding YQ (2011) Distribution of Satb1 in the central nervous system of adult mice. Neurosci Res 71(1):12–21. https://doi.org/10.1016/j.neures.2011.05.015

Husband S, Shimizu T (1999) Efferent projections of the ectostriatum in the pigeon (Columba livia). J Comp Neurol. https://doi.org/10.1002/(SICI)1096-9861(19990412)406:3

Jarvis E, Güntürkün O, Bruce L, Csillag A, Karten H, Kuenzel W, Medina L, Paxinos G, Perkel DJ, Shimizu T, Striedter G, Wild M, Ball J, Dugas-Ford GF, Durand J, Hough SE, Husband GE, Kubikova S, Lee L, Butler DW, A. B (2005) Avian brains and a new understanding of vertebrate brain evolution. Nat Rev Neurosci 6(2):151–159. https://doi.org/10.1038/NRN1606

Jarvis ED, Yu J, Rivas MV, Horita H, Feenders G, Whitney O, Jarvis SC, Jarvis ER, Kubikova L, Puck AEP, Siang-Bakshi C, Martin S, McElroy M, Hara E, Howard J, Pfenning A, Mouritsen H, Chen CC, Wada K (2013) Global view of the functional molecular organization of the avian cerebrum: mirror images and functional columns. J Comp Neurol 521(16):3614–3665. https://doi.org/10.1002/CNE.23404

Kepecs A, Fishell G (2014) Interneuron Cell Types: Fit to form and formed to fit. Nature 505(7483):318. https://doi.org/10.1038/nature12983

Lozano D, López JM, Jiménez S, Morona R, Ruíz V, Martínez A, Moreno N (2023) Expression of SATB1 and SATB2 in the brain of bony fishes: what fish reveal about evolution. Brain Struct Function 228(3–4):921. https://doi.org/10.1007/s00429-023-02632-z

Mascagni F, McDonald AJ (2003) Immunohistochemical characterization of cholecystokinin containing neurons in the rat basolateral amygdala. Brain Res 976(2):171–184. https://doi.org/10.1016/S0006-8993(03)02625-8

Medalla M, Mo B, Nasar R, Zhou Y, Park J, Luebke JI (2023) Comparative Features of Calretinin, Calbindin and Parvalbumin Expressing Interneurons in Mouse and Monkey Primary Visual and Frontal Cortices. J Comp Neurol 531(18):1934. https://doi.org/10.1002/cne.25514

Medina L, Reiner A (2000) Do birds possess homologues of mammalian primary visual, somatosensory and motor cortices? Trends Neurosci 23(1):1–12. https://doi.org/10.1016/S0166-2236(99)01486-1

Mitra S, Basu S, Singh O, Srivastava A, Singru PS (2022) Calcium-binding proteins typify the dopaminergic neuronal subtypes in the ventral tegmental area of zebra finch, Taeniopygia guttata. J Comp Neurol 530(14):2562–2586. https://doi.org/10.1002/CNE.25352

Mulder J, Zilberter M, Spence L, Tortoriello G, Uhlén M, Yanagawa Y, Aujard F, Hökfelt T, Harkany T (2009) Secretagogin is a Ca2+-binding protein specifying subpopulations of telencephalic neurons. Proc Natl Acad Sci 106(52):22492–22497. https://doi.org/10.1073/pnas.0912484106

Nasir-Ahmad S, Vanstone KA, Novelli M, Lee SCS, Do MTH, Martin PR, Grünert U (2021) Satb1 expression in retinal ganglion cells of marmosets, macaques and humans. J Comp Neurol 530(6):923. https://doi.org/10.1002/CNE.25258

Pai EL-L, Vogt D, Hu JS, Rubenstein JL (2024) Transcriptional Regulation of Cortical Interneuron Development. Jasper's Basic Mech Epilepsies. https://doi.org/10.1093/med/9780197549469.003.0047

Pitkänen A, Kemppainen S (2002) Comparison of the distribution of calcium-binding proteins and intrinsic connectivity in the lateral nucleus of the rat, monkey, and human amygdala. Pharmacol Biochem Behav 71(3):369–377. https://doi.org/10.1016/S0091-3057(01)00690-6

Puelles L, Martínez de la Torre M, Martinez S, Watson C, Paxinos G (2018) The chick brain in stereotaxic coordinates and alternate stains, 2nd edn. Academic

Reiner A, Perkel DJ, Bruce LL, Butler AB, Csillag A, Kuenzel W, Medina L, Paxinos G, Shimizu T, Striedter G, Wild M, Ball GF, Durand S, Gütürkün O, Lee DW, Mello CV, Powers A, White SA, Hough G, Jarvis ED (2004) Revised nomenclature for avian telencephalon and some related brainstem nuclei. J Comp Neurol 473(3):377–414. https://doi.org/10.1002/CNE.20118

Schindelin J, Arganda-Carreras I, Frise E, Kaynig V, Longair M, Pietzsch T, Preibisch S, Rueden C, Saalfeld S, Schmid B, Tinevez JY, White DJ, Hartenstein V, Eliceiri K, Tomancak P, Cardona A (2012) Fiji: an open-source platform for biological-image

analysis. Nat Methods 9(7):676–682. https://doi.org/10.1038/NMETH.2019

Sheehan-Rooney K, Pálinkášová B, Eberhart JK, Dixon MJ (2010) A cross-species analysis of Satb2 expression suggests deep conservation across vertebrate lineages. Dev Dynamics: Official Publication Am Association Anatomists 239(12):3481. https://doi.org/10.1002/dvdy.22483

Stacho M, Ströckens F, Xiao Q, Güntürkün O (2016) Functional organization of telencephalic visual association fields in pigeons. Behav Brain Res 303:93–102. https://doi.org/10.1016/j.bbr.2016.01.045

Stringer C, Wang T, Michaelos M, Pachitariu M (2020) Cellpose: a generalist algorithm for cellular segmentation. Nat Methods 2020 18(1):100–106. https://doi.org/10.1038/s41592-020-01018-x

Suárez J, Dávila JC, Ángeles Real M, Guirado S, Medina L (2006) Calcium-binding proteins, neuronal nitric oxide synthase, and GABA help to distinguish different pallial areas in the developing and adult chicken. I. Hippocampal formation and hyperpallium. J Comp Neurol 497(5):751–771. https://doi.org/10.1002/CNE.21004

Tosches MA, Yamawaki TM, Naumann RK, Jacobi AA, Tushev G, Laurent G (2018) Evolution of pallium, hippocampus, and cortical cell types revealed by single-cell transcriptomics in reptiles. Science 360(6391):881–888. https://doi.org/10.1126/science.aar4237

Turovsky EA, Tarabykin VS, Varlamova EG (2023) Deletion of the Neuronal Transcription Factor Satb1 Induced Disturbance of the Kinome and Mechanisms of Hypoxic Preconditioning. Biology 12(9):1207. https://doi.org/10.3390/biology12091207

Unal G, Joshi A, Viney TJ, Kis V, Somogyi P (2015) Synaptic targets of medial septal projections in the hippocampus and extrahippocampal cortices of the mouse. J Neurosci 35(48):15812–15826. https://doi.org/10.1523/JNEUROSCI.2639-15.2015

Viney TJ, Lasztoczi B, Katona L, Crump MG, Tukker JJ, Klausberger T, Somogyi P (2013) Network state-dependent inhibition of identified hippocampal CA3 axo-axonic cells in vivo. Nat Neurosci 16(12):1802–1811. https://doi.org/10.1038/NN.3550

von Eugen K, Tabrik S, Güntürkün O, Ströckens F (2020) A comparative analysis of the dopaminergic innervation of the executive caudal nidopallium in pigeon, chicken, zebra finch, and carrion crow. J Comp Neurol 528(17):2929–2955. https://doi.org/10.1002/CNE.24878

Wild JM, Williams MN, Howie GJ, Mooney R (2005) Calcium-binding proteins define interneurons in HVC of the zebra finch (Taeniopygia guttata). J Comp Neurol 483(1):76–90. https://doi.org/10.1002/CNE.20403

Wonders CP, Anderson SA (2006) The origin and specification of cortical interneurons. Nat Rev Neurosci 7(9):687–696. https://doi.org/10.1038/NRN1954

Xu Q, Tam M, Anderson SA (2008) Fate mapping Nkx2.1-lineage cells in the mouse telencephalon. J Comp Neurol 506(1):16–29. https://doi.org/10.1002/CNE.21529;JOURNAL:JOURNAL:15507130;PAGE:STRING:ARTICLE/CHAPTER

Zaremba B, Fallahshahroudi A, Schneider C, Schmidt J, Sarropoulos I, Leushkin E, Berki B, Van Poucke E, Jensen P, Senovilla-Ganzo R, Hervas-Sotomayor F, Trost N, Lamanna F, Sepp M, García-Moreno F, Kaessmann H (2025) Developmental origins and evolution of pallial cell types and structures in birds. Science. https://doi.org/10.1126/SCIENCE.ADP5182/SUPPL_FILE/SCIENCE.ADP5182_DATA_S1_TO_S4.ZIP

Zeier H, Karten HJ (1971) The archistriatum of the pigeon: Organization of afferent and efferent connections. Brain Res 31(2):313–326. https://doi.org/10.1016/0006-8993(71)90185-5

Zhang R, Long JL, Ye YF, Ye HY, Zhao XN, Cai X, Lu L (2025) Distributions of parvalbumin, calbindin-D28k, and calretinin in the cerebrum of Chinese tree shrews (Tupaia belangeri chinensis): A high-resolution neuroanatomical resource. Zoological Res 46(4):893. https://doi.org/10.24272/j.issn.2095-8137.2025.095

**Publisher's Note** Springer Nature remains neutral with regard to jurisdictional claims in published maps and institutional affiliations.

Springer Nature or its licensor (e.g. a society or other partner) holds exclusive rights to this article under a publishing agreement with the author(s) or other rightsholder(s); author self-archiving of the accepted manuscript version of this article is solely governed by the terms of such publishing agreement and applicable law.